

NACA TN 3865

CASE FILE
COPY

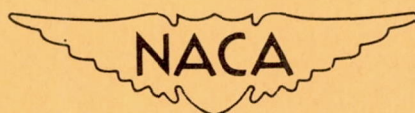
NATIONAL ADVISORY COMMITTEE FOR AERONAUTICS

TECHNICAL NOTE 3865

WIND-TUNNEL INVESTIGATION OF JET-AUGMENTED FLAPS ON A
RECTANGULAR WING TO HIGH MOMENTUM COEFFICIENTS

By Vernard E. Lockwood, Thomas R. Turner,
and John M. Riebe

Langley Aeronautical Laboratory
Langley Field, Va.



Washington

December 1956

NATIONAL ADVISORY COMMITTEE FOR AERONAUTICS

TECHNICAL NOTE 3865

WIND-TUNNEL INVESTIGATION OF JET-AUGMENTED FLAPS ON A
RECTANGULAR WING TO HIGH MOMENTUM COEFFICIENTS

By Vernard E. Lockwood, Thomas R. Turner,
and John M. Riebe

SUMMARY

A preliminary investigation of jet flaps has been made in the 300 MPH 7- by 10-foot tunnel on an unswept, untapered wing with an aspect ratio of 8.4 and a thickness of 16.7 percent. A jet of air was blown backward through a small gap, tangentially to the upper surface of a round trailing edge, and was separated from the trailing edge at various angles up to 110° with respect to the wing chord line. In addition, a limited number of tests were made of a jet-augmented plain flap and a jet-augmented trim flap.

The results of the investigation showed that the ratio of total lift to jet-reaction lift increased as the jet deflection angle increased and reached a maximum value for jet deflections of 86° and 110°. Although the jet-circulation lift coefficient increased as the momentum coefficient increased in the low momentum-coefficient range, the ratio of jet-circulation lift to jet momentum decreased; for example, with the jet deflected 86° the ratio of circulation lift to momentum varied from a value of 10 at a momentum coefficient of 0.2 (lift coefficient of 2.3) to a value of 1.2 at a momentum coefficient of 7 (lift coefficient of 16). The induced-drag coefficients were materially less over the momentum-coefficient range from 0.5 to 14 than would be obtained from the formula

$$\frac{(\text{Circulation lift coefficient})^2}{\pi(\text{Aspect ratio})}$$

The jet flap gave large pitching-moment coefficients with respect to the 27.6-percent-chord line. For the 86° jet at an angle of attack of 0°, these coefficients varied from about 0.5 to 6.25 for a momentum-coefficient range from 0.2 to 7.0. A limited amount of data showed that it is possible to reduce the pitching moments of the jet flap by the addition of a split-flap arrangement for directing the line of action of the jet through the center of moments, but at the expense of additional drag.

INTRODUCTION

Investigations of wings and flaps that use high-pressure air as a boundary-layer-control device for the attainment of theoretical lift effectiveness have shown that the increase of lift coefficient with momentum coefficient has continued into the range of momentum coefficients beyond those necessary for flow attachment. Although the rate of increase of lift coefficient with momentum coefficient above the lift coefficient for flow attachment is less than that prior to flow attachment, the lift-coefficient increase is still several times that of the momentum-coefficient increase. Consideration of this fact, coupled with the continued need for more powerful high-lift aids, has resulted in an extension of blowing-flap research into the high momentum-coefficient range. This work has indicated that for the condition of high momentum it is not necessary to provide the airfoil with a flap, since the deflected jet of air provides the increase in lift coefficient. This system has been called a jet flap. The results of a two-dimensional experimental investigation up to a momentum coefficient of about 4.2 are given in reference 1, and the results of a three-dimensional investigation on a wing with an aspect ratio of 3 are given in reference 2.

The present investigation was made in the Langley 300 MPH 7- by 10-foot tunnel to obtain some basic data on the jet flap which can be applied to the design of STOL (short take-off and landing) aircraft. A rectangular wing with an aspect ratio of 8.4 and a thickness of 16.7 percent (the forward portion of a basic NACA 0012 airfoil section) was used to study the effects of a jet flap on the aerodynamic characteristics of the wing up to momentum coefficients of about 56. (For this investigation the jet of air was ejected backward over the upper surface of a round trailing edge, to which it clung by means of the Coanda effect until it separated naturally or at a desired angle fixed by means of a wedge.) In addition, a limited investigation was made of a jet blowing over the upper surface of a plain flap (hereinafter called the jet-augmented plain flap) and also a jet flap in combination with a split flap attached to the lower surface of the wing so as to reduce the reaction moments of the jet (hereinafter called the jet-augmented trim flap).

This paper also contains an estimation of the low-flight velocities that might be expected of a hypothetical airplane using the jet-flap system investigated.

The effects of aspect ratio have been investigated on jet-flap wings similar to the one used in the present investigation and the results are presented in reference 3.

SYMBOLS

The coefficients of forces and moments are referred to the wind axes with the center of moments at 27.6 percent of the mean aerodynamic chord.

A	aspect ratio
C_D	drag coefficient, $Drag/qS$
C_L	lift coefficient, $Lift/qS$
$(C_L)_\Gamma$	jet-circulation lift coefficient
C_m	pitching-moment coefficient, $M/S\bar{c}q$
C_μ	momentum coefficient, $w_j V_j / gqS$
\bar{c}	mean aerodynamic chord of wing, 0.603 ft (with jet-augmented plain flap, 0.833 ft)
e	a form of Oswald's efficiency factor appearing in the induced-drag equation, $C_{D,i} = \frac{(C_L)_\Gamma^2}{e\pi A}$
g	acceleration due to gravity, ft/sec ²
M	pitching moment, ft-lb
p	free-stream static pressure, lb/sq ft
p_p	total pressure in plenum chamber, lb/sq ft
q	free-stream dynamic pressure, $\rho V^2/2$, lb/sq ft
R	universal gas constant
S	wing area, 1.508 sq ft (with jet-augmented plain flap, 2.083 sq ft)
T	plenum-chamber temperature, deg Rankine
V	free-stream velocity, ft/sec

V_j	jet velocity (isentropic expansion is assumed), $\sqrt{\frac{2\gamma}{\gamma-1} RTg \left[1 - \left(\frac{p}{p_p} \right)^{\frac{\gamma-1}{\gamma}} \right]}, \text{ ft/sec}$
w_j	weight rate of flow of jet, lb/sec
x	distance from center of moments to line of action of jet
α	angle of attack of wing chord line
α_t	angle of attack of model with respect to tunnel center line
γ	ratio of specific heats for air, 1.4
δ	jet-deflection angle, measured with respect to wing chord line
ρ	mass density of air, slugs/cu ft
Subscripts:	
i	induced
o	profile

APPARATUS AND MODEL

The jet-flap investigation was made in the Langley 300 MPH 7-by 10-foot tunnel by means of the semispan technique with the ceiling of the tunnel as the reflection plane. The general arrangement of the wing and the jet-flap configurations tested are shown in figure 1. The jet-flap wing was constructed by removing the rear 30 percent of a 10-inch-chord wing that had NACA 0012 airfoil sections and installing a 0.750-inch-diameter tube and a plenum chamber, as shown in figure 1. High-pressure air was brought in through the tube and ejected into the wing plenum chamber through 59 holes of 1/16-inch diameter located in the tube at spanwise intervals of one-half inch. For the jet-flap configurations, wedges were attached to the trailing edge of the wing to fix the angle δ that the resulting jet made with the wing chord line. The slight increase of wing area resulting from addition of the wedges was not considered a part of the basic wing area. The trailing-edge portion of the wing removed for construction of the jet-flap configurations was used to make the jet-augmented plain-flap configuration. A wooden wedge and steel plate were used for construction of the jet-augmented trim-flap configuration. (See fig. 2.)

The compressed air was brought onto the balance frame through a $1\frac{1}{2}$ -inch-diameter steel pipe (fig. 3). One end of the long pipe was fastened rigidly to the tunnel foundation and the other end was attached rigidly to the balance frame. The pipe was long enough to be considered as a very weak spring connecting the balance frame to the ground. The tare of this setup was determined experimentally to be within the accuracy of reading of the scales.

The weight rate of flow of air was determined by means of a calibrated sharp-edge orifice in the pipe line before the air came onto the balance frame, and the pressures and temperatures for determining the jet-exit velocities were measured in the plenum chamber in the wing.

TEST CONDITIONS

The tests were made in the Langley 300 MPH 7- by 10-foot tunnel at the dynamic pressures, velocities, Mach numbers, and Reynolds numbers given in the following table:

Dynamic pressure, q, lb/sq ft	Velocity, V, ft/sec	Reynolds number	Mach number	Momentum coefficient, C_μ
0.56	21.8	84,000	----	56.75
1.13	30.8	119,000	----	28.5
2.26	43.7	168,000	----	14.37
4.5	61.7	238,000	----	7.1
8.5	84.7	326,000	----	0, 1.96, 0.15 to 4.5
16.9	119.7	460,000	0.11	0.96
110.6	340	1,230,000	.30	0 and 0.079
164.2	373	1,300,000	.33	0.008 to 0.058

Included in the table are the momentum coefficients that were investigated at each dynamic pressure. The momentum coefficients at the highest dynamic pressures were lower because of the limited air supply available. The angle-of-attack range for the investigation extended from -12° to about 20° .

CORRECTIONS

Jet-boundary corrections applied to the data were obtained by the methods of reference 4. The magnitudes of the corrections were determined

by considering only the aerodynamic forces (circulation-lift effects) on the model that resulted after the jet-reaction components had been subtracted from the data as follows:

$$\alpha = \alpha_t + 0.142 [C_L - C_\mu \sin(\delta + \alpha)]$$

$$C_D = (C_D)_{\text{measured}} + 0.0025 [C_L - C_\mu \sin(\delta + \alpha)]^2$$

Blocking corrections have not been applied to the data because they were believed to be negligible in view of the small size of the model with respect to the tunnel test section.

PRESENTATION OF RESULTS

The results of the investigation are presented in the following figures:

	Figure
Calibration of the nozzle	4
Aerodynamic characteristics in pitch	5 to 11
Aerodynamic characteristics at $\alpha = 0^\circ$	12 and 13
Factors making up lift	14 to 16
Aerodynamic characteristics in pitch at high dynamic pressures; $\delta = 86^\circ$	17
Induced-drag factor	18
Factors making up pitch	19 and 20
Comparison of aerodynamic characteristics of jet flap, jet-augmented trim flap, and jet-augmented plain flap	21
Thrust required for low-speed flight of a hypothetical jet-flap airplane	22

DISCUSSION

A brief discussion of the momentum coefficient is necessary because the data presented are dependent upon the basis used for calculating this coefficient. The momentum coefficient used herein is based upon the product of the mass of air discharged through the slot and the theoretical velocity obtained by assuming isentropic expansion to free-stream static pressure. In a converging nozzle, efficiencies of nearly 100 percent are obtained up to choking velocity, above which a slight loss occurs as

the pressure ratio is increased. The nozzle used in the present investigation is shown in figures 1 and 2 and the calibration of the 57° and 86° jet nozzles is shown in figure 4. (Several values of the ratio of plenum-chamber pressure to free-stream static pressure that existed for the calibration are indicated in the figure.) These data indicate that the measured reaction is approximately 75 percent of the calculated value for either jet angle. It should be emphasized that the theoretical momentum coefficient has been used in analyzing these data because it is believed that the momentum of the jet at the nozzle exit is largely responsible for the change in circulation around the wing, and because the losses in the jet due to overexpanding, turning, and base pressure could not be individually evaluated from the results of these data.

Jet Flap

Lift coefficient.— The lift coefficient of a wing with a jet flap can be divided into three components as indicated in figure 14 and as summed up in the following expression:

$$C_L = (C_L)_{C_\mu=0} + C_\mu \sin(\delta + \alpha) + (C_L)_\Gamma$$

where $(C_L)_{C_\mu=0}$ is the jet-off lift coefficient or the lift coefficient of a wing resulting from camber or angle of attack with no blowing. The term $C_\mu \sin(\delta + \alpha)$ is the component of the momentum coefficient in the lift direction and is hereinafter referred to as the reaction lift coefficient. The reaction lift is directly proportional to the momentum, as is indicated by the straight line in figure 14. The term $(C_L)_\Gamma$ is the pressure-lift coefficient induced by the jet sheet and is referred to as the jet-circulation lift coefficient. The data of this figure (which are for the 86° jet deflection) show that the jet-circulation lift increases very rapidly with increase of momentum in the low momentum-coefficient range, but in the higher momentum range the rate is considerably reduced. As an example, consider ratios of $(C_L)_\Gamma$ to C_μ at relatively low and high values of C_μ . At $C_\mu = 0.2$ ($C_L \approx 2.3$) the ratio of $(C_L)_\Gamma$ to C_μ is about 10 to 1, whereas at $C_\mu = 7.0$ ($C_L \approx 16$) the ratio is 1.2 to 1.

The lift effectiveness of the jet flap at various deflections is given in figure 15. In this figure the ratio of total lift coefficient C_L to the component of momentum coefficient in the lift direction $C_\mu \sin \delta$ is presented against C_μ for an angle of attack of 0°. These data show that the lift effectiveness is a function of the jet-deflection angle, as the values of the magnification factor $C_L / (C_\mu \sin \delta)$ are

smallest for the 28° jets and greatest for the 86° and 110° jets. Values of the magnification factor vary from 32 at $C_\mu = 0.008$ to about 1.4 at $C_\mu = 29.0$ for the 86° jet deflection. Although the data of figure 15 indicate that the lift is some function of flap deflection, this fact is better illustrated in figure 16 where the circulation-lift coefficient has been determined for several momentum coefficients and is shown to be approximately proportional to the jet-deflection angle. This result should be expected by use of plain-flap analogy.

The lift-curve slopes of the various jet-deflection angles (figs. 5 to 9) show large variations through the momentum-coefficient and jet-deflection ranges. From the lift equation presented previously, if the jet-circulation lift is independent of angle of attack, the lift-curve slope C_{L_α} per degree is

$$C_{L_\alpha} = (C_{L_\alpha})_{C_\mu=0} + \frac{C_\mu \cos(\delta + \alpha)}{57.3}$$

This equation accounts for the change in lift-curve slope C_{L_α} with momentum coefficient and the reduction in C_{L_α} as δ increases (figs. 5 to 9). This reduction in C_{L_α} is graphically illustrated for the jet deflection of 110° , where the value of C_{L_α} becomes negative at large values of C_μ (fig. 9). The variation of stalling angle of attack with momentum coefficient is of interest. Figures 6 to 11, and particularly figure 8, show that as the momentum coefficient is increased to about 2 the stalling angle of attack generally decreases; further increases of momentum coefficient result in increasing angle of stall, however.

Drag.—As this investigation was primarily intended to determine the lift potentialities of a jet flap, little attention was given to drag in the design; consequently the minimum drag coefficient of this configuration is high. The minimum drag coefficient for the 86° jet configuration at $C_\mu = 0$ is approximately 0.040 (fig. 17), which is in agreement with the calculated value from reference 5 for a wing of this thickness and bluntness.

The drag can be divided into its components as follows:

$$C_D = C_{D,o} + C_\mu \cos(\delta + \alpha) + C_{D,i}$$

where $C_{D,o}$ is the profile-drag coefficient at zero lift and $C_\mu \cos(\delta + \alpha)$ is the component of the jet in the drag direction. The part of the equation which is of principal interest in this investigation is the induced drag

$$C_{D,i} = \frac{(C_L)_\Gamma^2}{\pi A}$$

where e is an induced-drag efficiency factor similar to that used in reference 6 and A is the geometric aspect ratio. The factor e accounts for any variation of drag other than the direct component of the momentum; it can include such items as the deviation from elliptical loading, the variation of profile drag with lift, drag resulting from any low-pressure region at the base of the wing, and the induced thrust, if any, which varies according to $C_\mu(1 - \cos \delta)$ as discussed in reference 1. The values of e have been calculated for the 86° jet flap at $\alpha = 0^\circ$ for a range of momentum coefficients from 0.5 to 56.8 (fig. 18). A value of e of about 0.85 is considered average for a wing of this plan form. Values of e greater than 0.85 are indicative of smaller induced drags. The values of e for the 86° jet flap increase from 0.86 at $C_\mu = 0.5$ to a maximum value of 1.25 at $C_\mu = 5.0$ and thereafter decrease to a value of about 0.65 at $C_\mu = 56.8$. The induced drags based on these values of e for a momentum-coefficient range from 0.5 to 14 are materially less than would be ordinarily calculated from the induced-drag equation.

Pitching moment.— The pitching-moment coefficients are given with respect to a point 27.6 percent rearward of the leading edge. At zero momentum the aerodynamic center is at the quarter-chord station, as measured over the lift range given in figure 17. As the momentum coefficient is increased to 0.079 the aerodynamic center moves rearward to about the 27-percent station. The data for the larger momentum coefficients, which were taken at low dynamic pressures, are not included, as the balance system was not sensitive enough to establish trends with angle of attack; hence, only the pitching moments resulting from changes in momentum coefficient at $\alpha = 0^\circ$ are presented.

The jet flap has large pitching moments, as would be expected from the jet reaction at the trailing edge of the wing. A typical example is the total pitching-moment coefficient for the 86° jet at $\alpha = 0^\circ$ (fig. 19). The pitching-moment coefficient varies from about -0.5 at $C_L = 2.3$ ($C_\mu = 0.2$) to -6.25 at $C_L = 16$ ($C_\mu = 7$). The reaction and jet-circulation components of the jet have been computed from the following equation:

$$C_m = (C_m)_{C_\mu=0} + C_\mu(\sin \delta)\frac{x}{c} + (C_m)_\Gamma$$

and it is found that the reaction component $C_\mu(\sin \delta)\frac{x}{c}$ varies from about $3/4$ to about 5 times the circulation component $(C_m)_\Gamma$ for lift coefficients from 2.3 to 16.

Jet-Augmented Trim Flap

One method of reducing the reaction moments is the jet-augmented trim flap shown in figure 2, based on a suggestion of Roger W. Griswold II. It consists of a jet flap with a plate attached to the bottom surface in such a manner as to direct the line of action of the jet leaving the wing through or near the center of moments. The data of figures 20 and 21 show a considerable reduction in pitching moment for the jet-augmented trim flap of figure 2(a) in comparison with the jet flap for the same jet deflection of 40° . For example, when C_L is about 40 the pitching-moment coefficient of the jet-augmented trim flap is about $1/3$ that of the jet flap (fig. 20). As would be expected, the reduction of pitching moments is not without cost, since the jet-augmented trim flap shows considerable increase in drag (fig. 21(b)). (The jet-augmented trim flap represents a flap that is retractable in the high-speed configuration, as these coefficients are based on the chord of the jet flap.)

Jet-Augmented Plain Flap

The jet-augmented plain flap was included in this investigation to obtain some effects of high momentum over a practical airfoil profile. The aspect ratio was reduced to 6.0 when the trailing edge was added to complete the airfoil contour, and the resulting jet deflection was 67° (the flap chord line was deflected 70°). The jet-augmented plain flap gave about the same lift and drag coefficients as the jet flap; however, the pitching-moment coefficients were materially smaller - about 70 per cent of the values for the jet flap - as shown in figure 21(c).

Estimated Thrust Required For Steady Flight of an

Airplane With the Jet-Flap System

A preliminary evaluation of a jet flap on an airplane, with regard to the thrust required for steady flight, has been made in order to illustrate the effect of jet-flap lift magnification on the steady-flight performance of an airplane. Figure 22 presents the estimated thrust required as a function of the velocity for a 75,000-pound airplane having a wing loading of 60 pounds per square foot and a plan form identical to the one investigated with the jet flap. The lift and momentum coefficients as a function of velocity are also included. In these calculations only the aerodynamic forces and moments of the wing as obtained directly from the tunnel data were considered. (The conditions assumed are ideal; such items as ground effect, stability change, and the effect of gusts have been neglected in the calculations.) The steady-flight system of thrust

balancing drag ($C_D = 0$) was obtained by varying the jet-deflection angle as shown by the upper curves of figure 22. The thrust-required curves are for the untrimmed pitching-moment condition and for the conditions in which diving moments for the jet flap were balanced by means of a jet download applied at $2\bar{c}$ rearward of the moment center and by a jet upload applied at $2\bar{c}$ ahead of the moment center. This figure indicates that the application of jet thrust ahead of the moment center on an airplane having a thrust-weight ratio of 0.5 would enable the airplane to maintain steady flight at approximately 38 knots, which corresponds to $C_L \approx 12$ and $C_\mu \approx 6$. This value is considerably lower than the landing or take-off velocity of a conventional airplane, which for an assumed value of $C_L = 2$ would be 94 knots. The larger total thrust required for the canard trim arrangement with respect to the untrimmed condition is attributed to the fact that part of the thrust applied in the lift direction is not under the influence of the jet-flap magnification effect. Use of a download applied at $2\bar{c}$ behind the moment center was found to be very costly in terms of thrust required for trim.

SUMMARY OF RESULTS

A preliminary investigation of a jet flap at low speed on an unswept, untapered wing with an aspect ratio of 8.4 and a thickness of 16.7 percent has yielded the following results:

1. The ratio of total lift to jet-reaction lift increased as the jet-deflection angle increased, and reached a maximum value for jet deflections of 86° and 110° .

2. Although the jet-circulation lift coefficient increased as the momentum coefficient increased in the low momentum-coefficient range, the ratio of jet-circulation lift to jet momentum decreased; for example, with the jet deflected 86° the ratio of circulation lift to momentum varied from a value of 10 at a momentum coefficient of 0.2 and a total lift coefficient of 2.3 to a value of 1.2 at a momentum coefficient of 7 and a total lift coefficient of 16.

3. The induced-drag coefficients were materially less over the momentum-coefficient range from 0.5 to 14 than would be given by the equation $(\text{Circulation lift coefficient})^2 / \pi(\text{Aspect ratio})$.

4. The jet flap gave large pitching-moment coefficients with respect to the 27.6-percent-chord line, which for the 86° jet at an angle of attack of 0° varied from about 0.5 to 6.25 for a momentum-coefficient range from 0.2 to 7.0. A limited amount of data showed that it is possible to reduce the pitching moments of the jet flap by the addition of a

split-flap arrangement for directing the line of action of the jet through the center of moments, but at the expense of additional drag.

Langley Aeronautical Laboratory,
National Advisory Committee for Aeronautics,
Langley Field, Va., September 4, 1956.

REFERENCES

1. Dimmock, N. A.: An Experimental Introduction to the Jet Flap. National Gas Turbine Establishment Rep. No. R.175, British Ministry of Supply, Apr. 1955.
2. Williams, J., and Alexander, A. J.: Three-Dimensional Wind-Tunnel Tests of a 30° Jet Flap Model. Rep. No. F.M. 2326, British N.P.L. (Rep. No. 17,990, A.R.C.), Nov., 1955.
3. Lowry, John G., and Vogler, Raymond D.: Wind-Tunnel Investigation at Low Speeds to Determine the Effect of Aspect Ratio and End Plates on a Rectangular Wing With Jet Flaps Deflected 85° . NACA TN 3863, 1956.
4. Gillis, Clarence L., Polhamus, Edward C., and Gray, Joseph L., Jr.: Charts for Determining Jet-Boundary Corrections for Complete Models in 7- by 10-Foot Closed Rectangular Wind Tunnels. NACA WR L-123, 1945. (Formerly NACA ARR L5G31.)
5. Hoerner, Sighard F.: Aerodynamic Drag. Publ. by the author (148 Busteed, Midland Park, N. J.), 1951.
6. Oswald, W. Bailey: General Formulas and Charts for the Calculation of Airplane Performance. NACA Rep. 408, 1932.

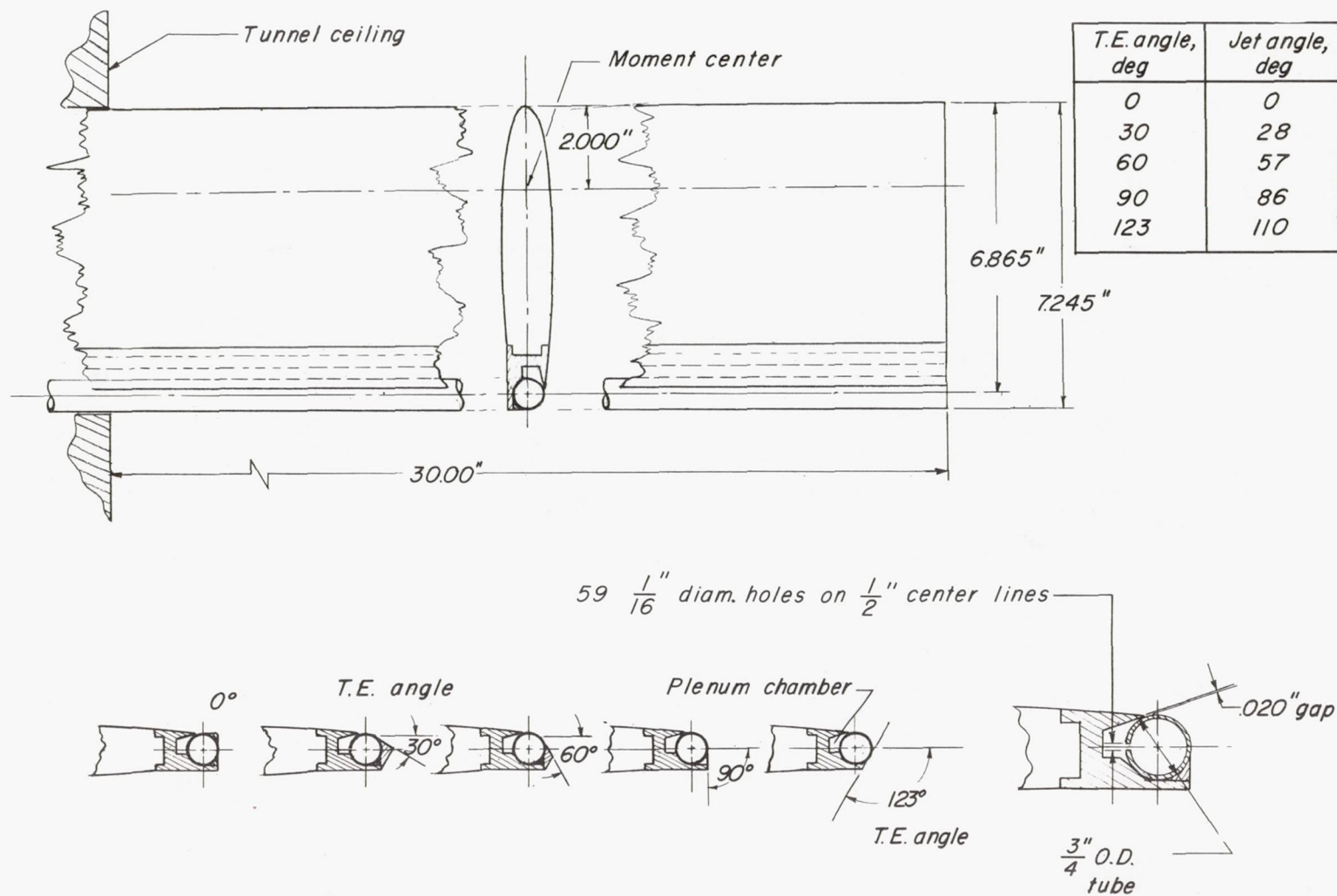
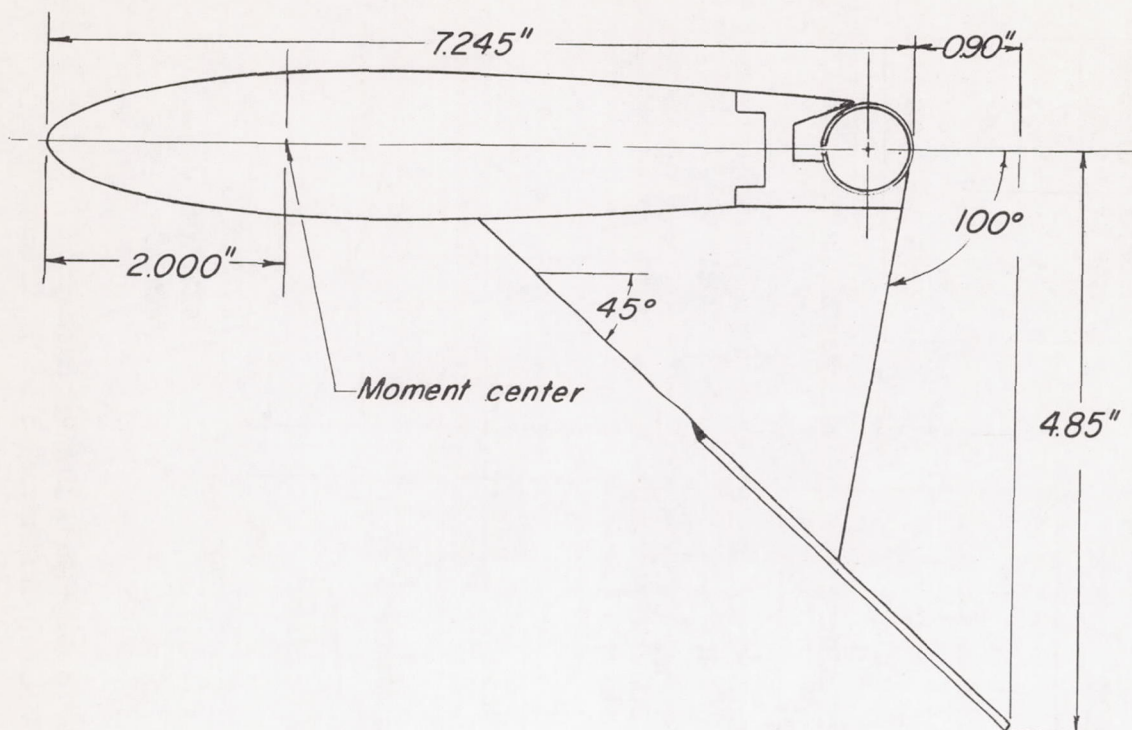
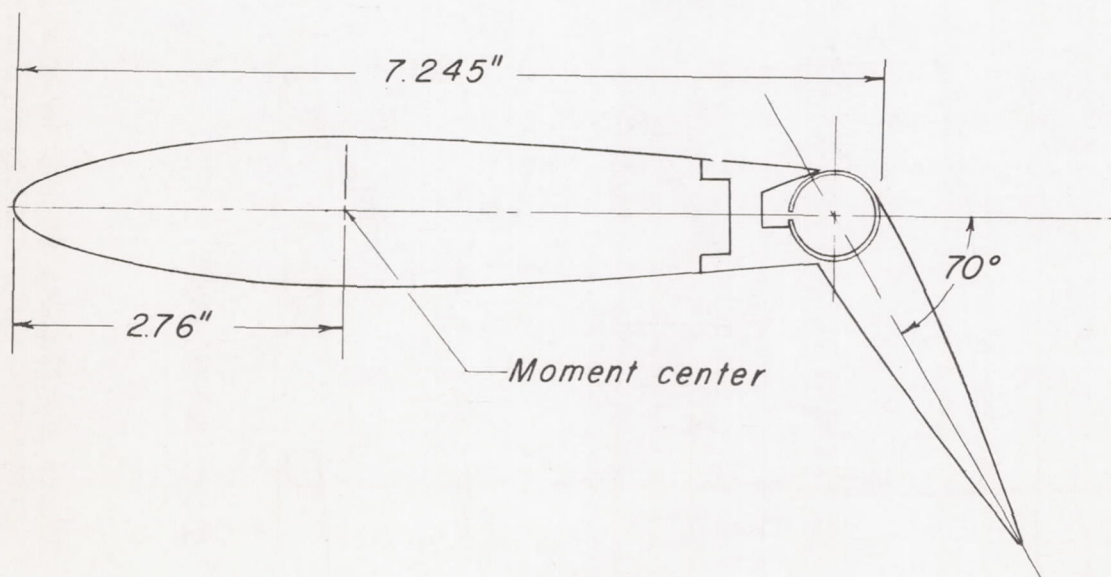


Figure 1.- Details of the jet-flap arrangement investigated on an unswept, untapered wing with an aspect ratio of 8.4 and a thickness of 16.7 percent.



(a) Jet-augmented trim flap. $\bar{c} = 7.245$ inches; jet angle, 40° .



(b) Jet-augmented plain flap. $\bar{c} = 10.00$ inches; jet angle, 67° .

Figure 2.- Details of the jet-augmented trim-flap and jet-augmented plain-flap arrangements investigated.

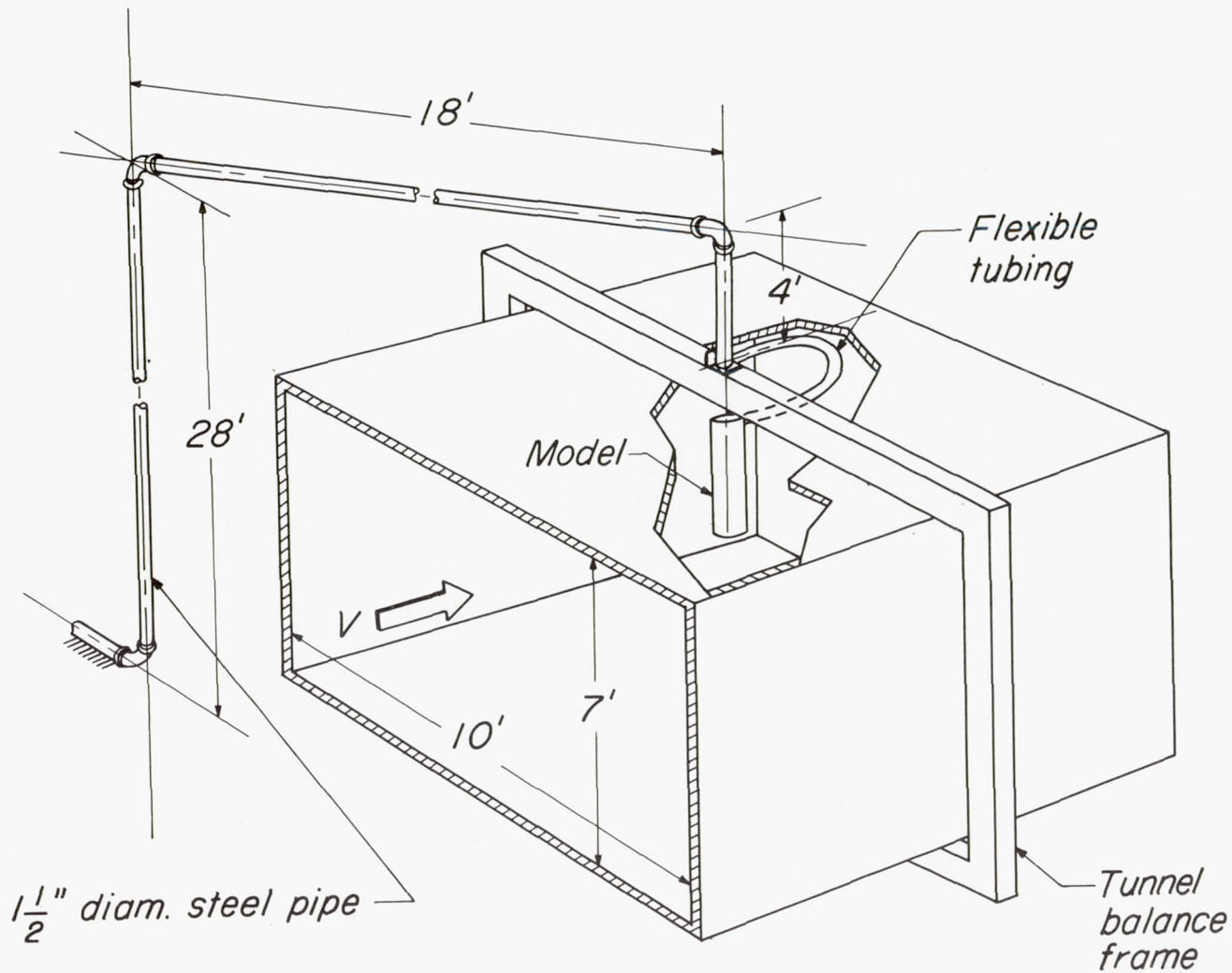


Figure 3.- Schematic diagram of the method used to introduce high-pressure air to model.

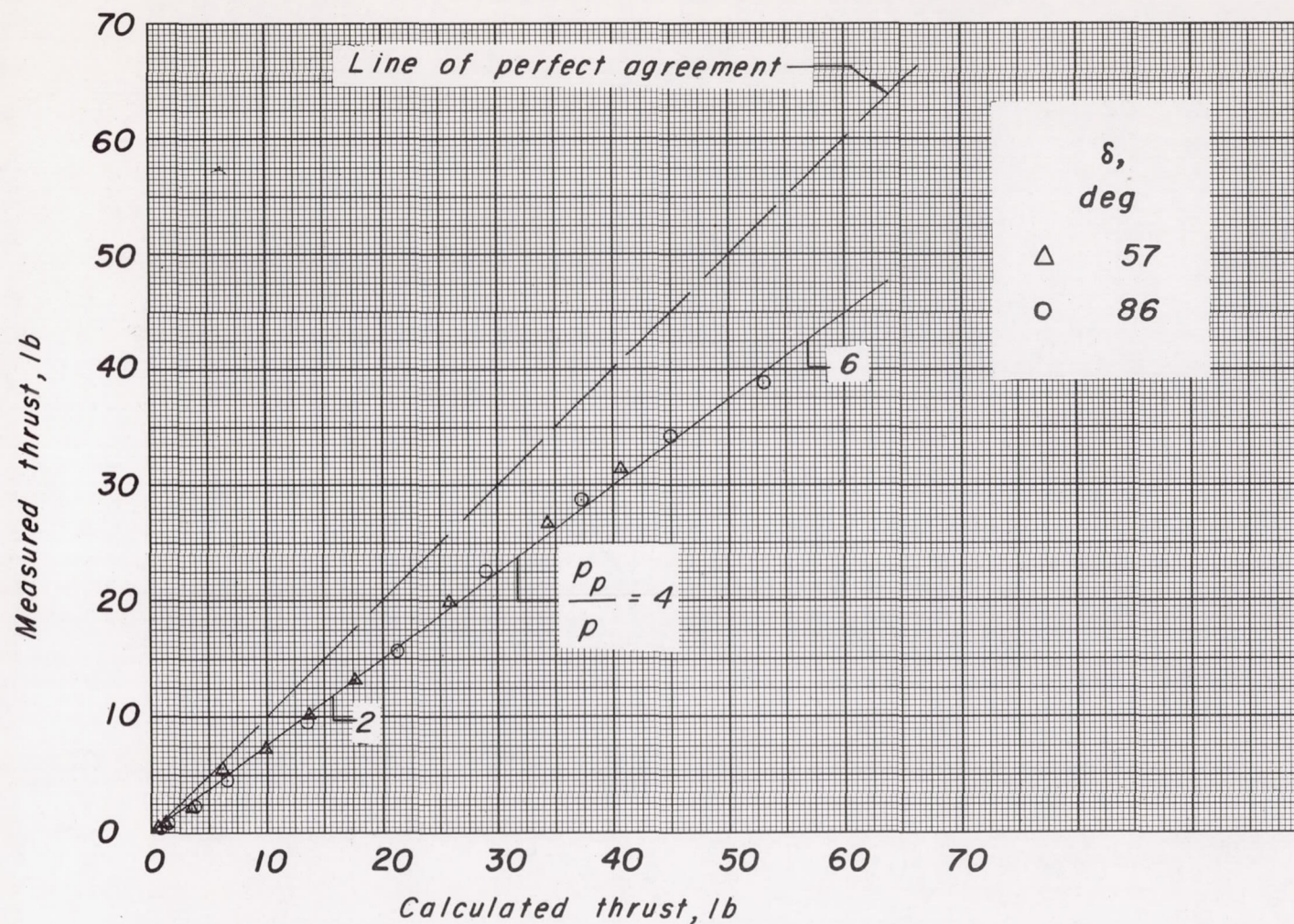


Figure 4.- Variation of calculated momentum with measured momentum for the 57° and 86° jet flaps. Numbers on figure indicate ratio of plenum-chamber pressure to free-stream static pressure.

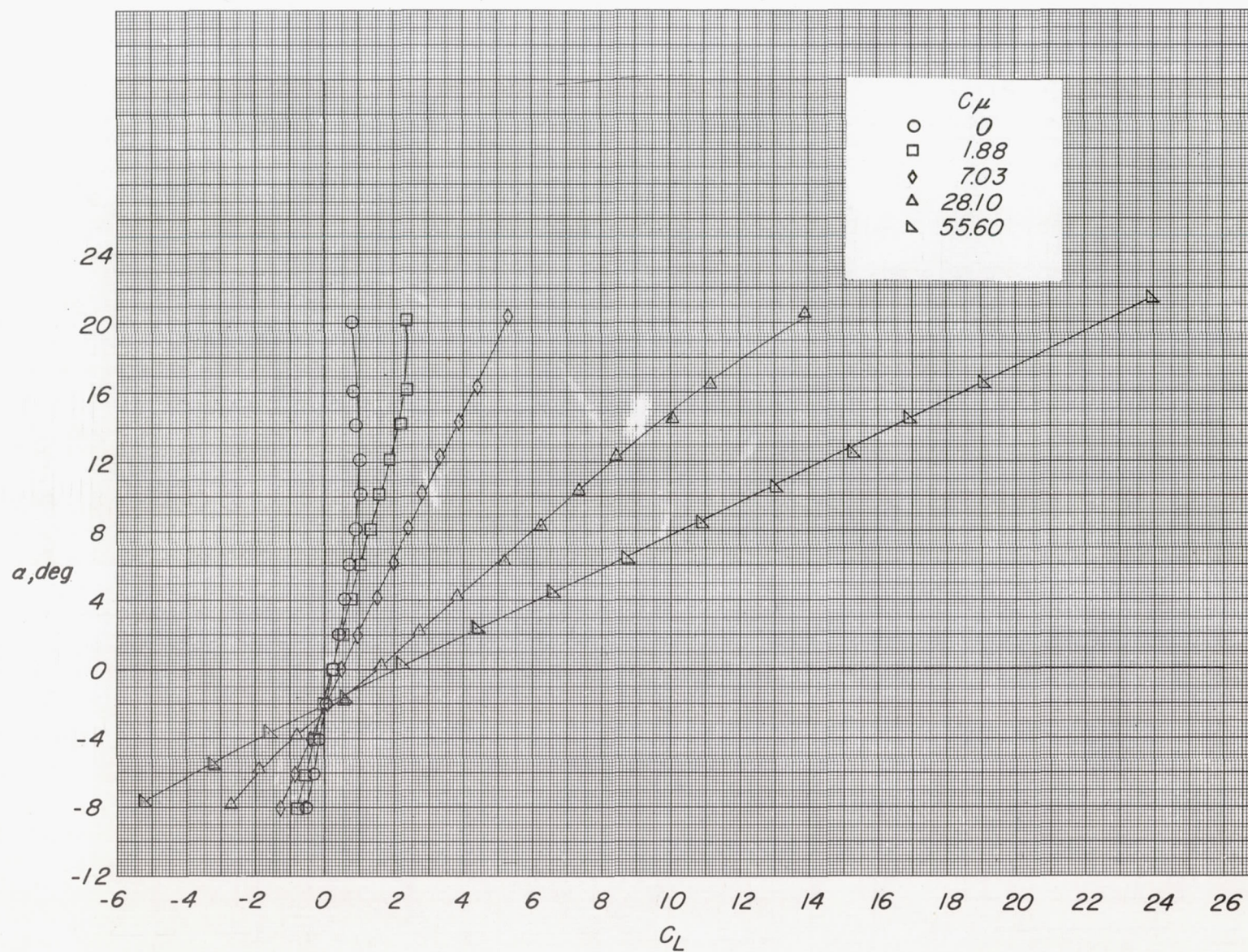


Figure 5.- Aerodynamic characteristics in pitch of the jet flap at $\delta = 0^\circ$.

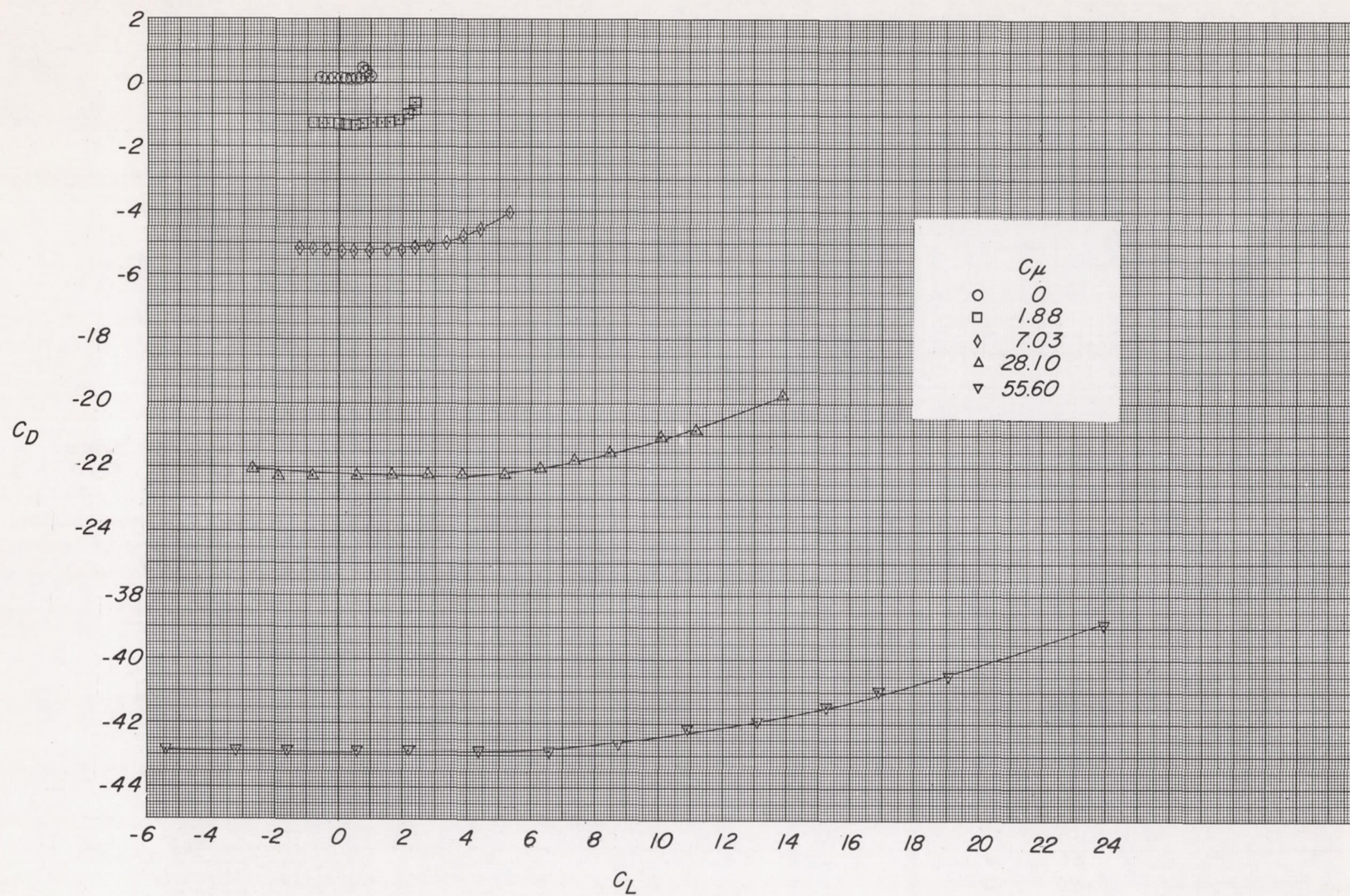


Figure 5.- Concluded.

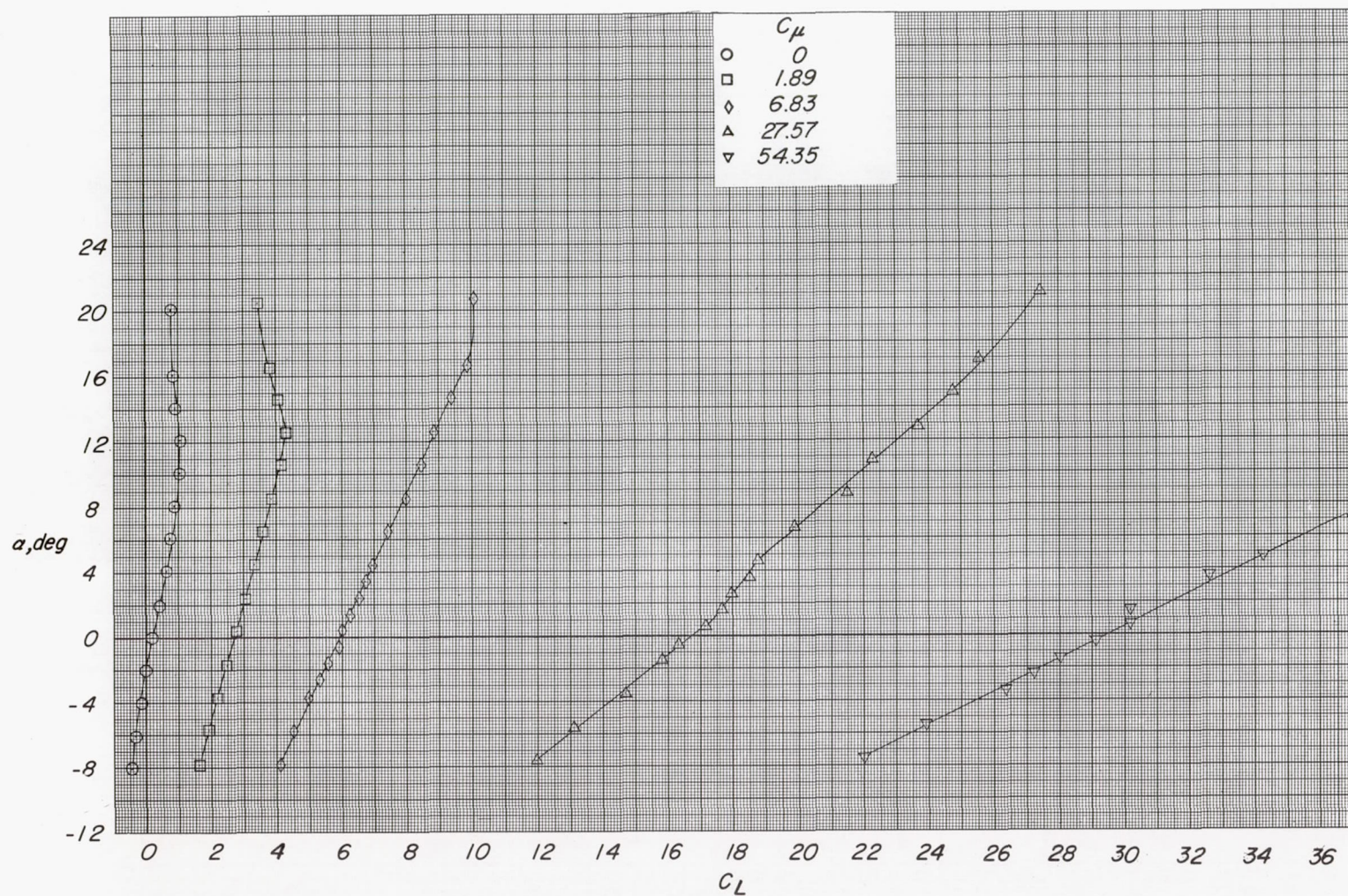


Figure 6.- Aerodynamic characteristics in pitch of the jet flap at $\delta = 28^\circ$.

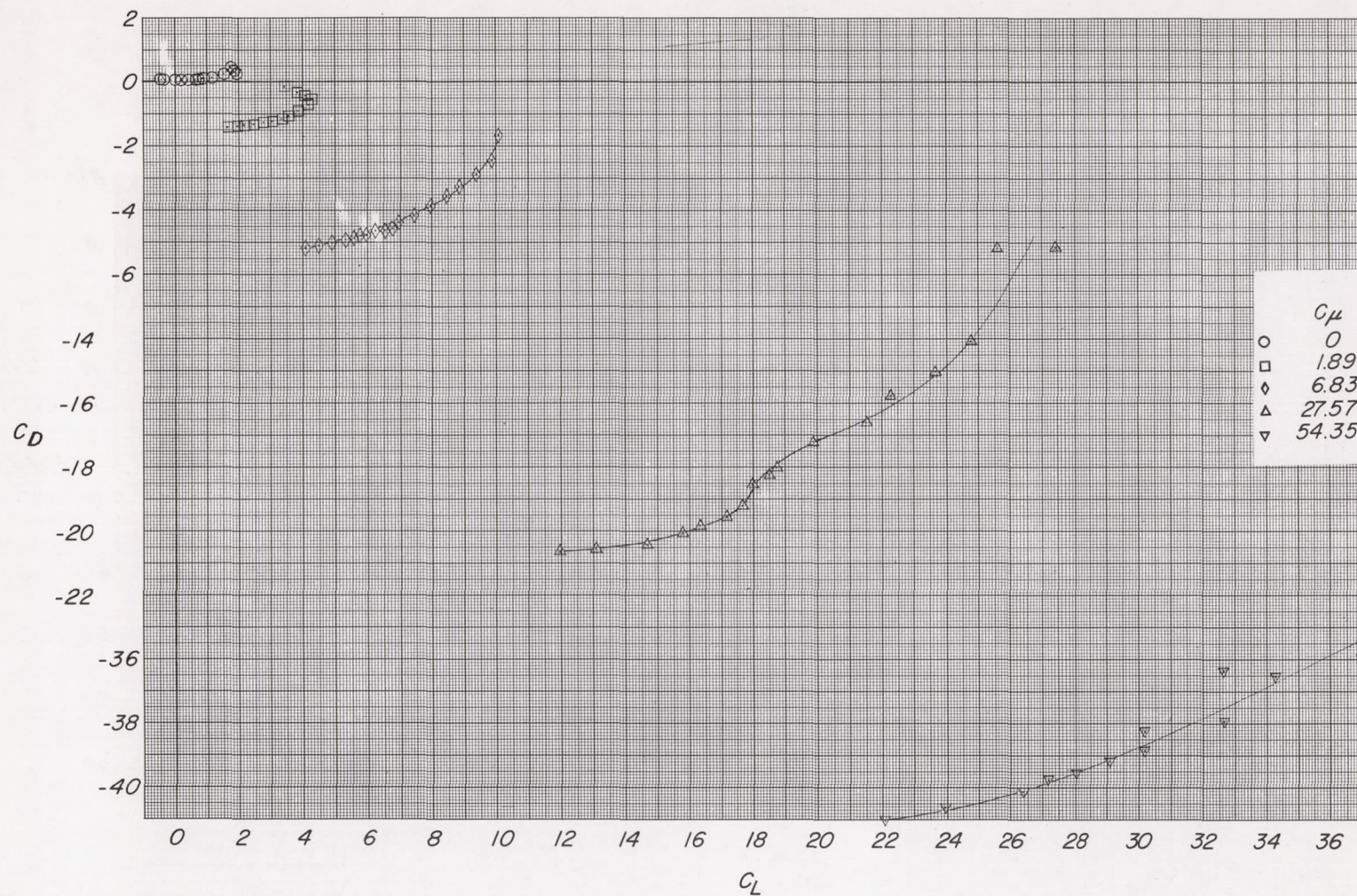


Figure 6.- Concluded.

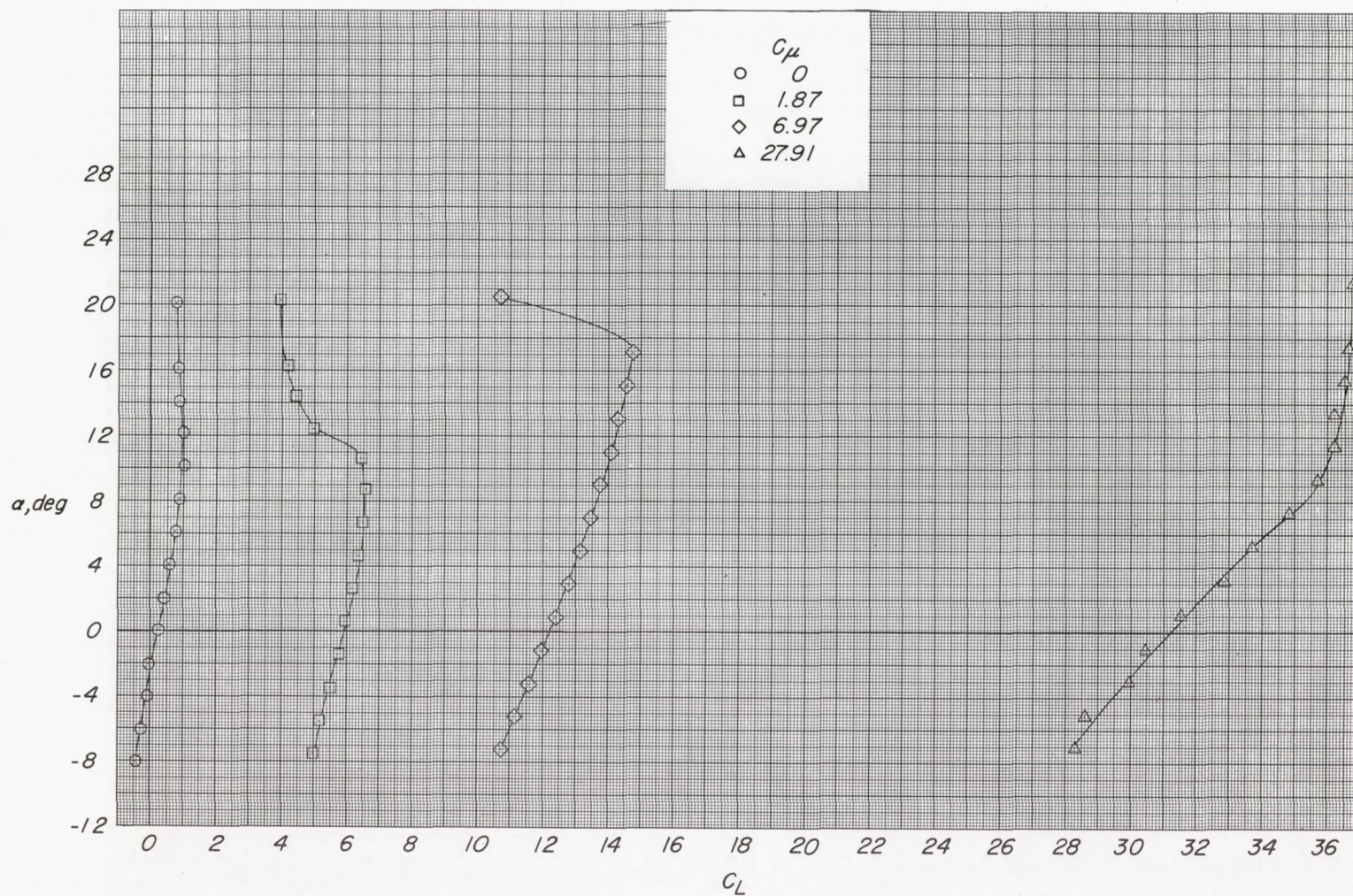


Figure 7.- Aerodynamic characteristics in pitch of the jet flap at $\delta = 57^\circ$.

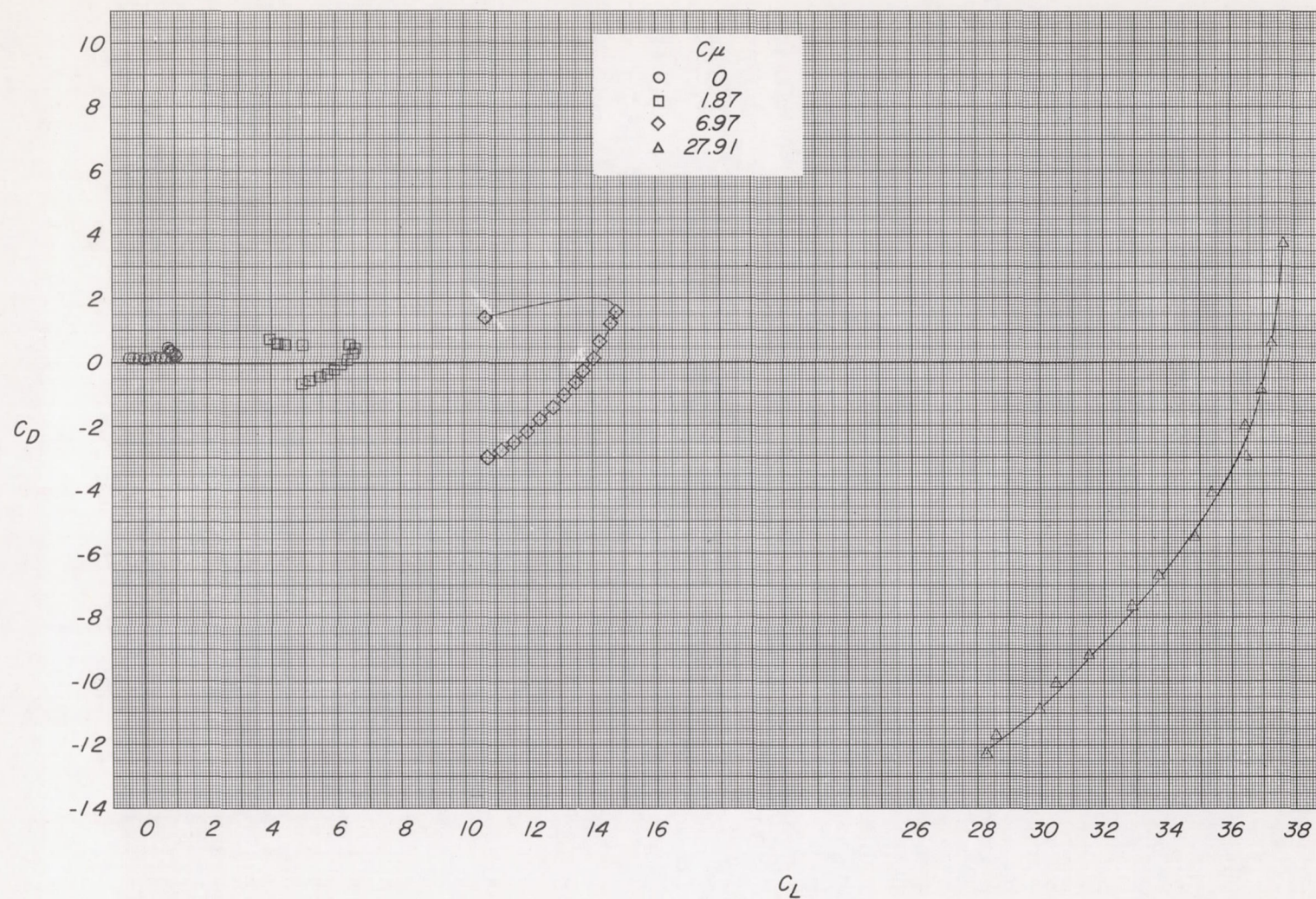


Figure 7.- Concluded.

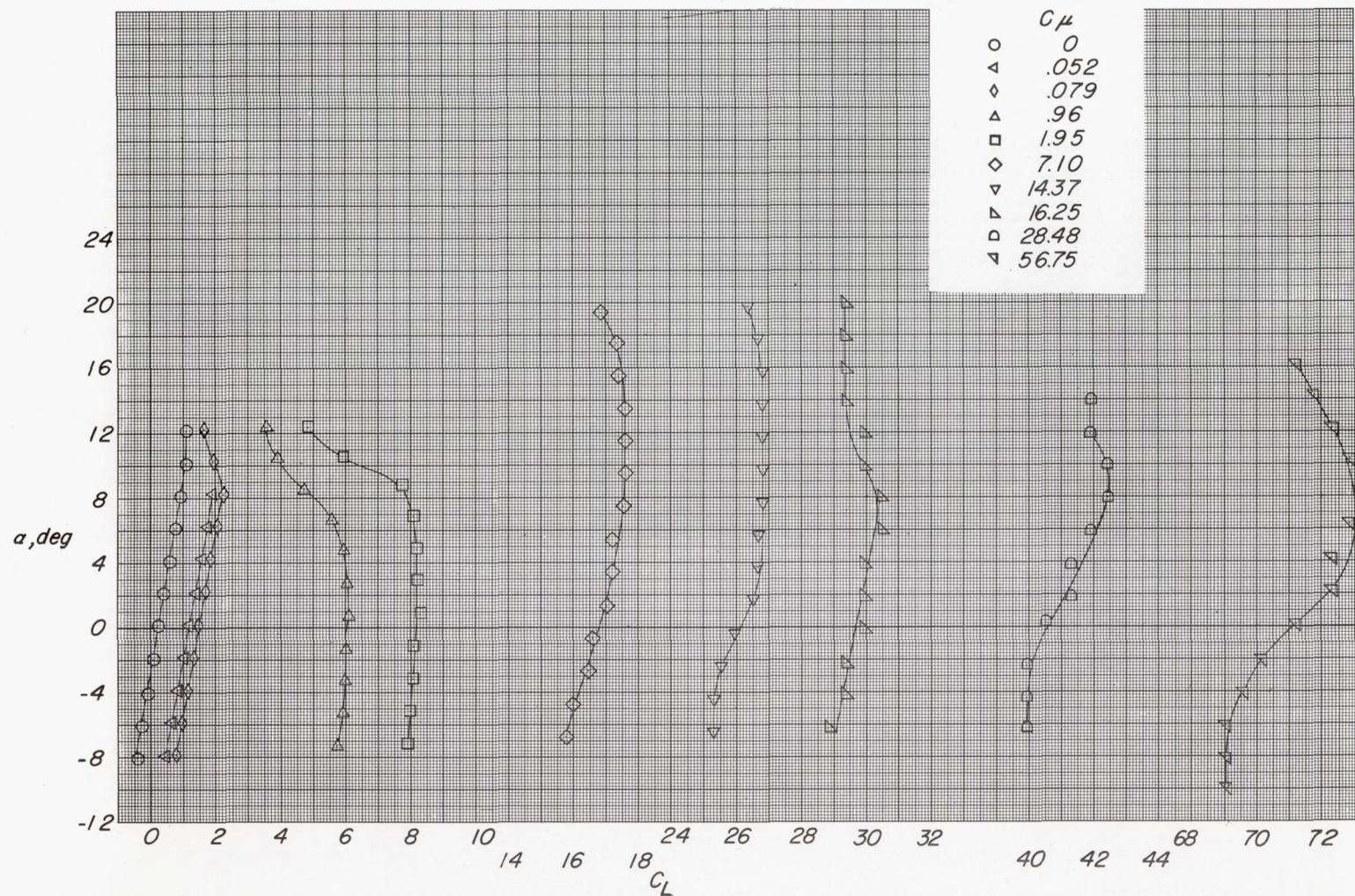


Figure 8.- Aerodynamic characteristics in pitch of the jet flap at $\delta = 86^\circ$.

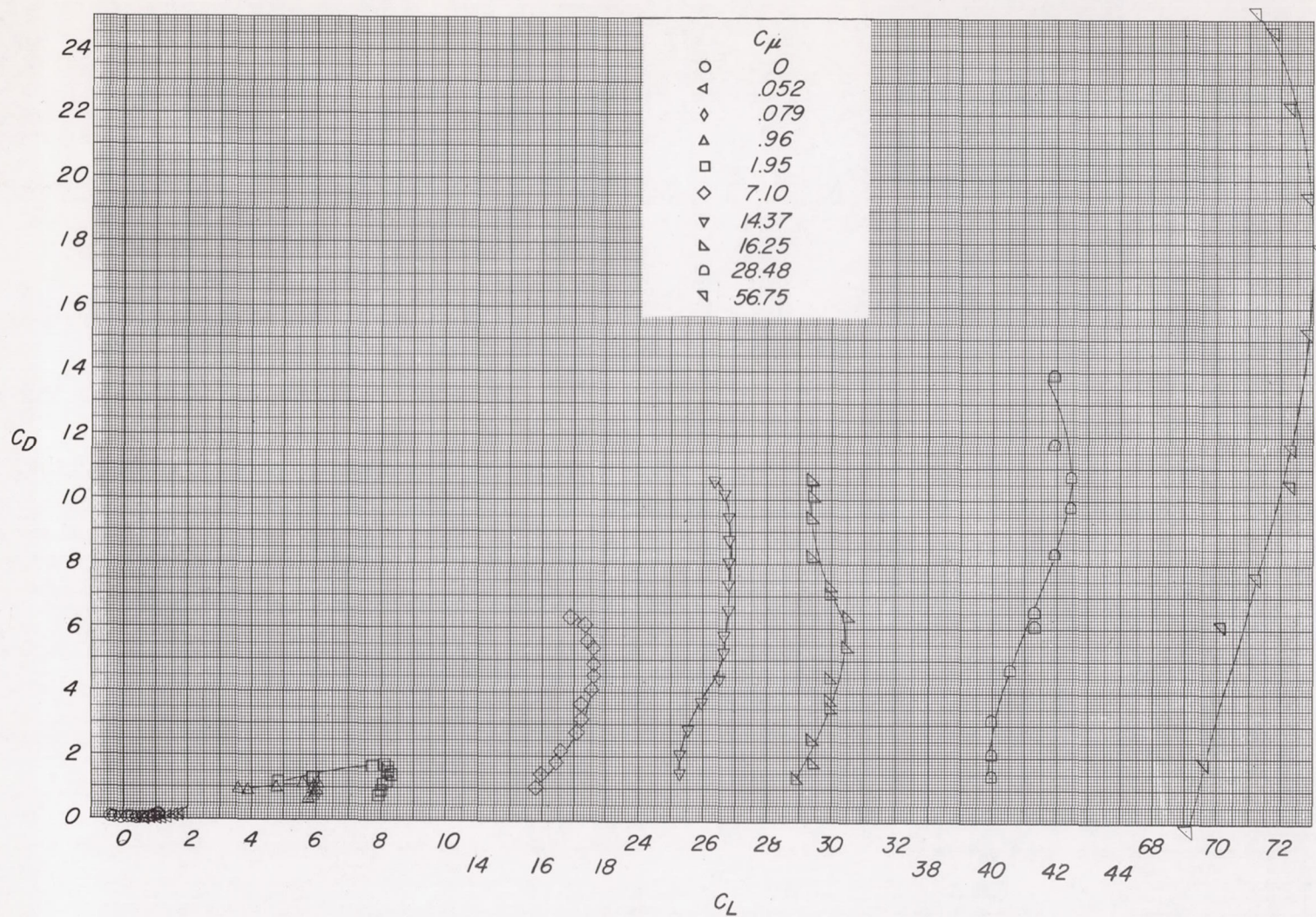


Figure 8.- Concluded.

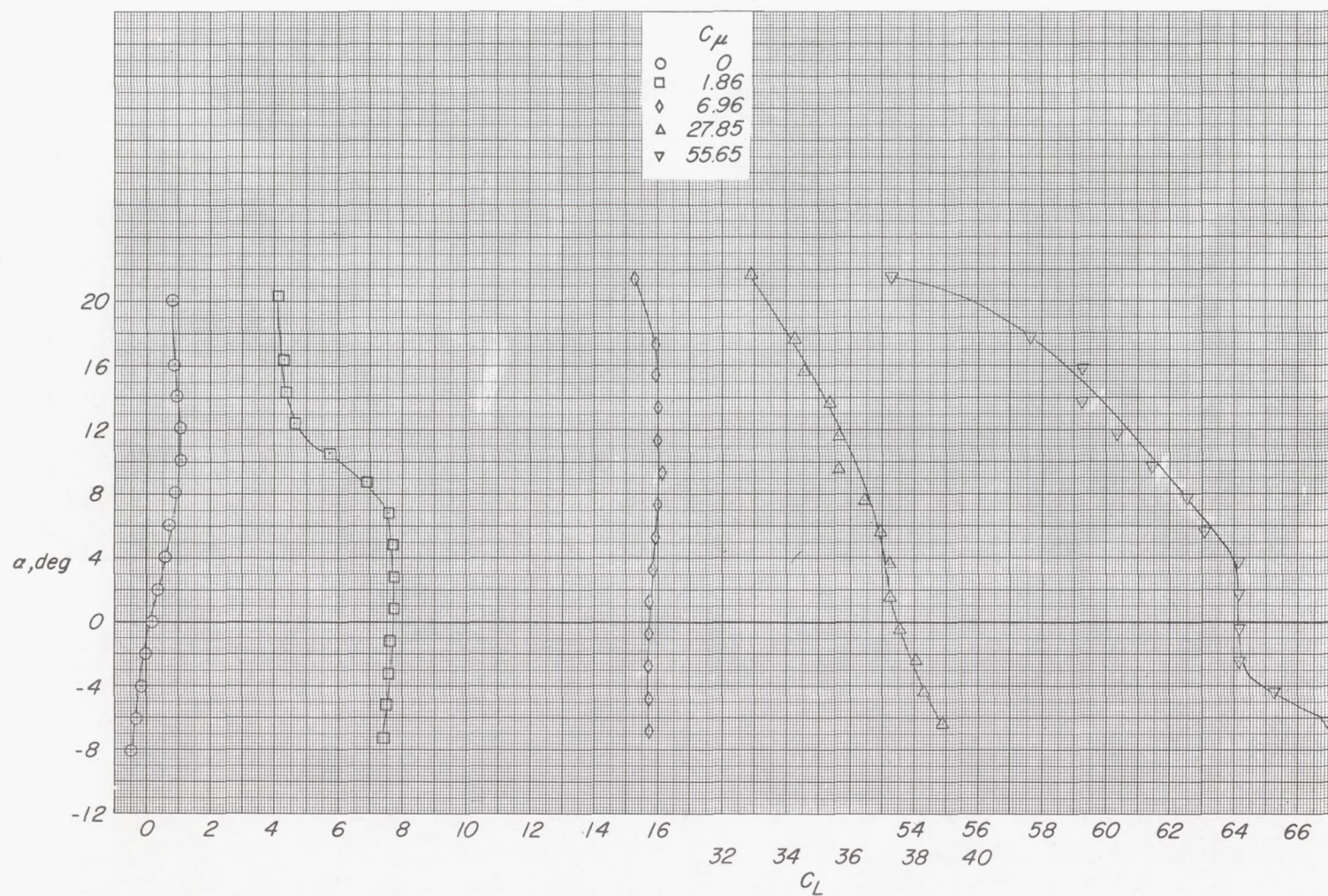


Figure 9.- Aerodynamic characteristics in pitch of the jet flap at $\delta = 110^\circ$.

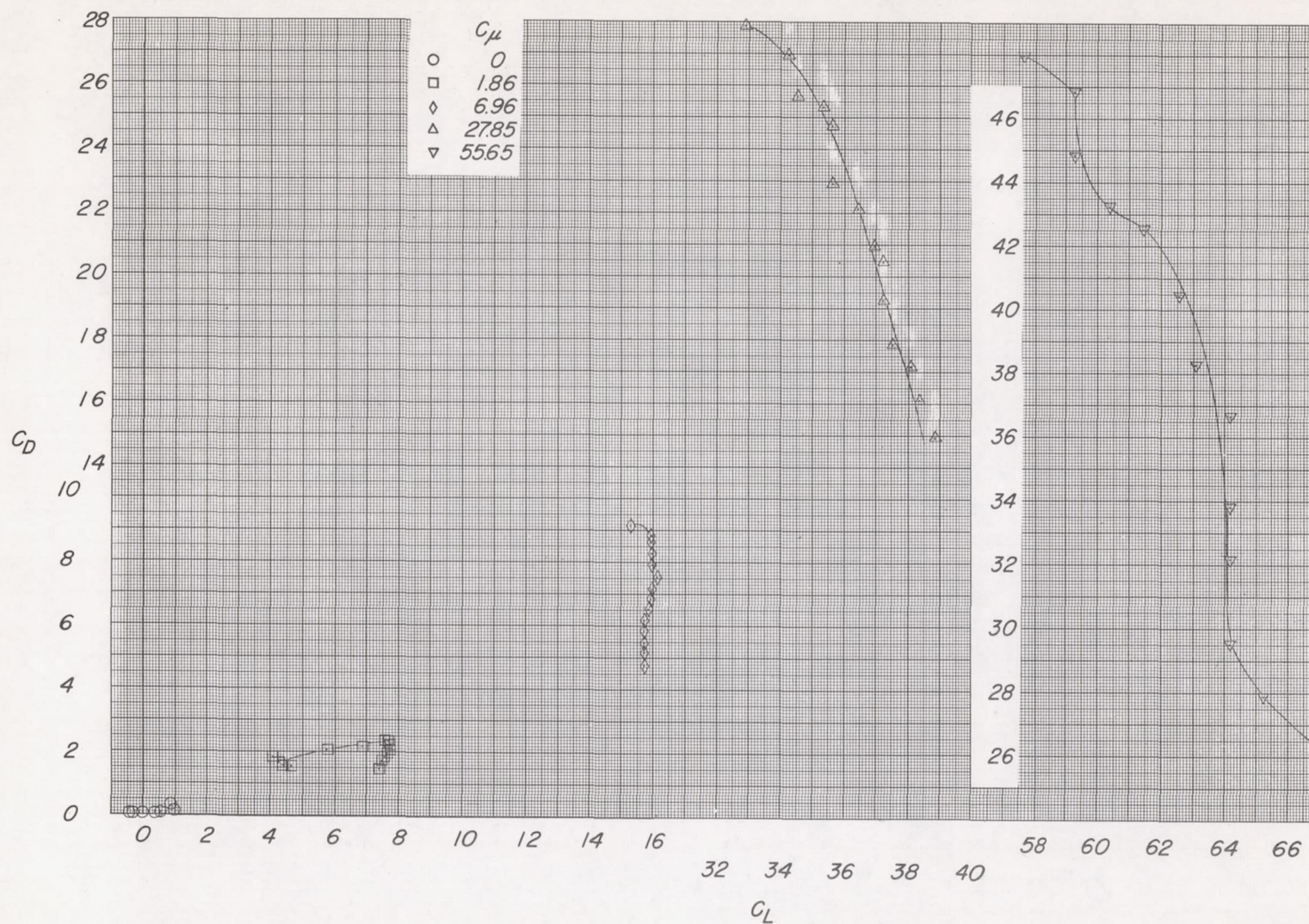


Figure 9.- Concluded.

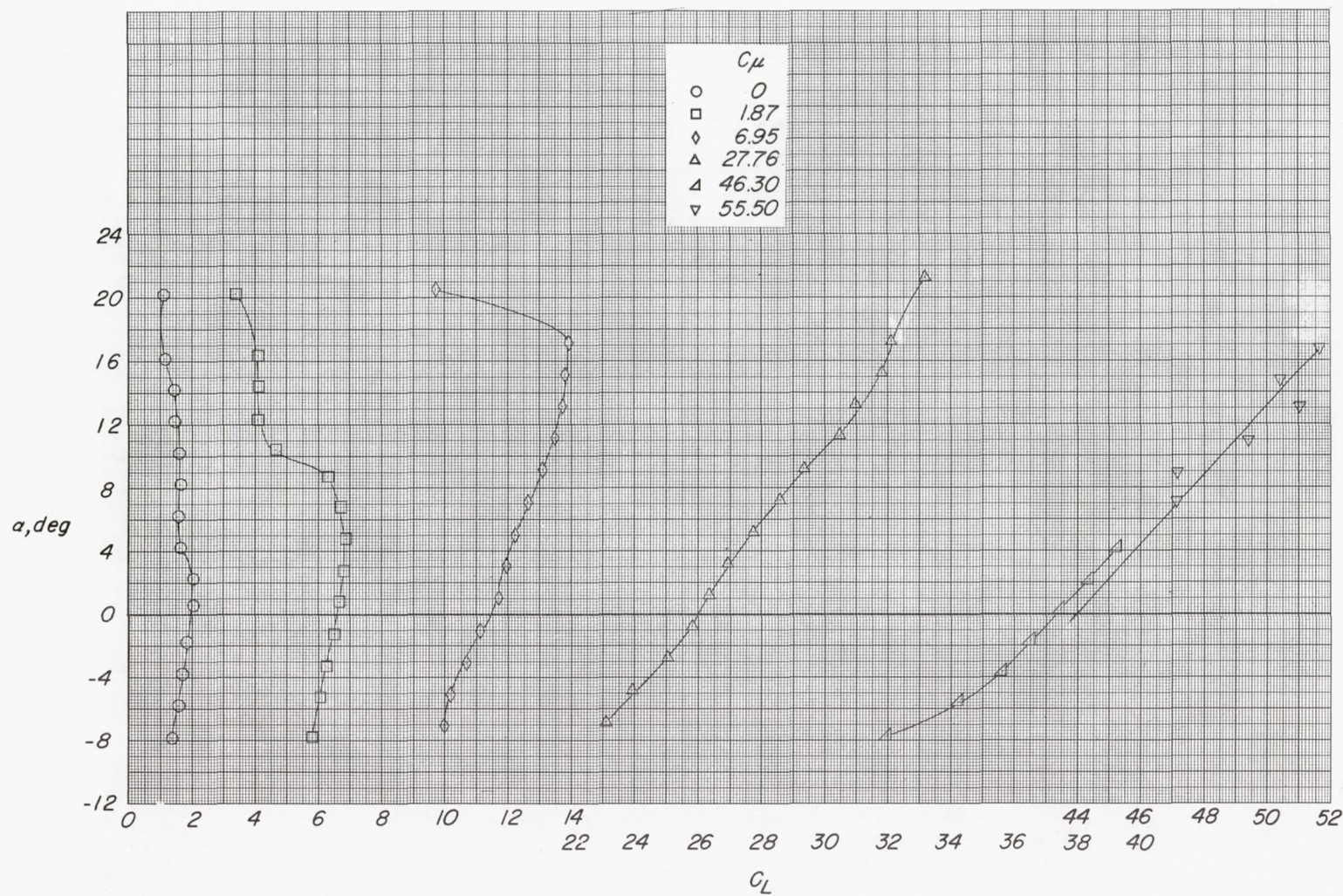


Figure 10.- Aerodynamic characteristics in pitch of the jet-augmented trim flap at $\delta = 40^\circ$.

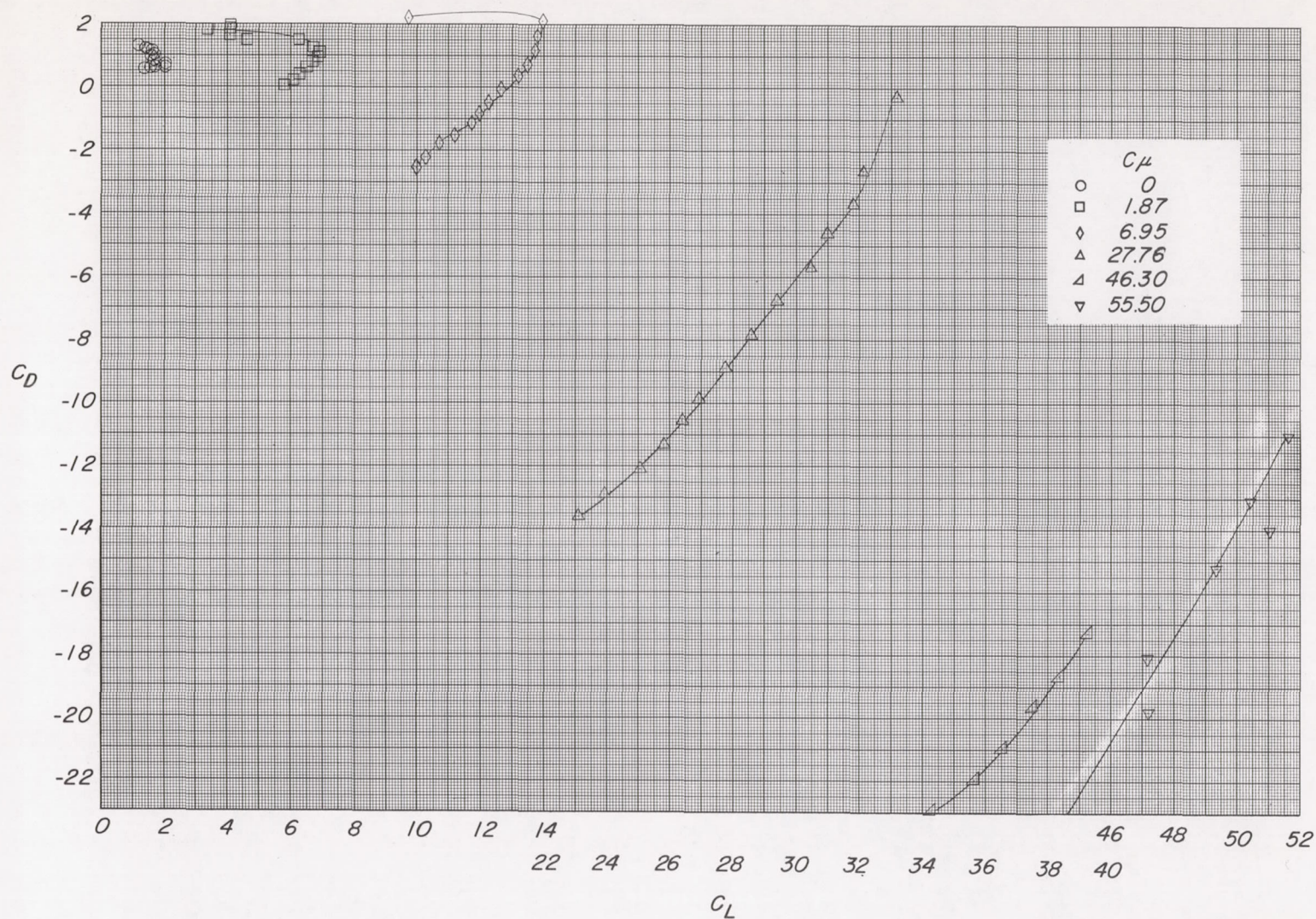


Figure 10.- Concluded.

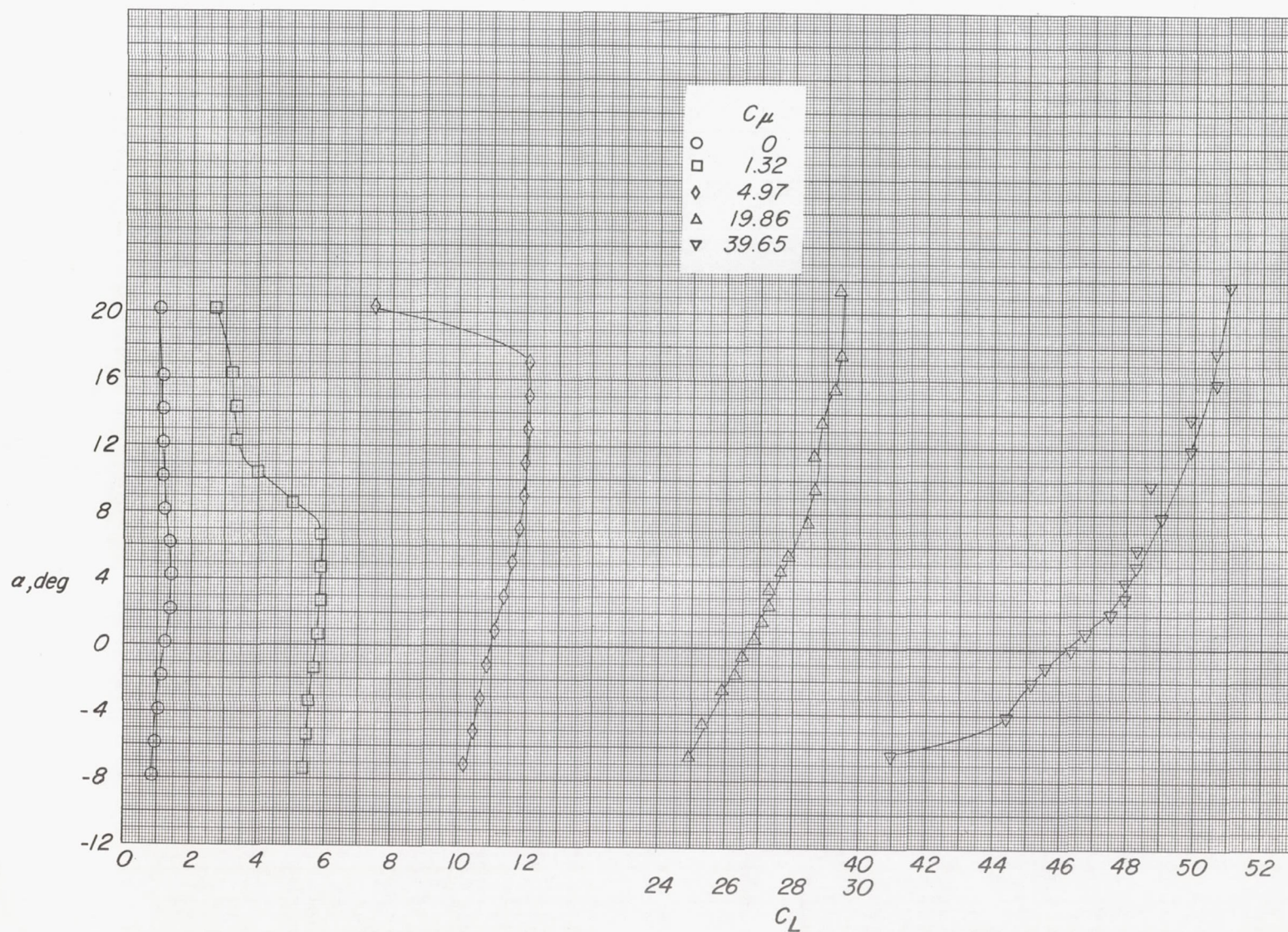


Figure 11.- Aerodynamic characteristics in pitch of the jet-augmented plain flap at $\delta = 67^\circ$.

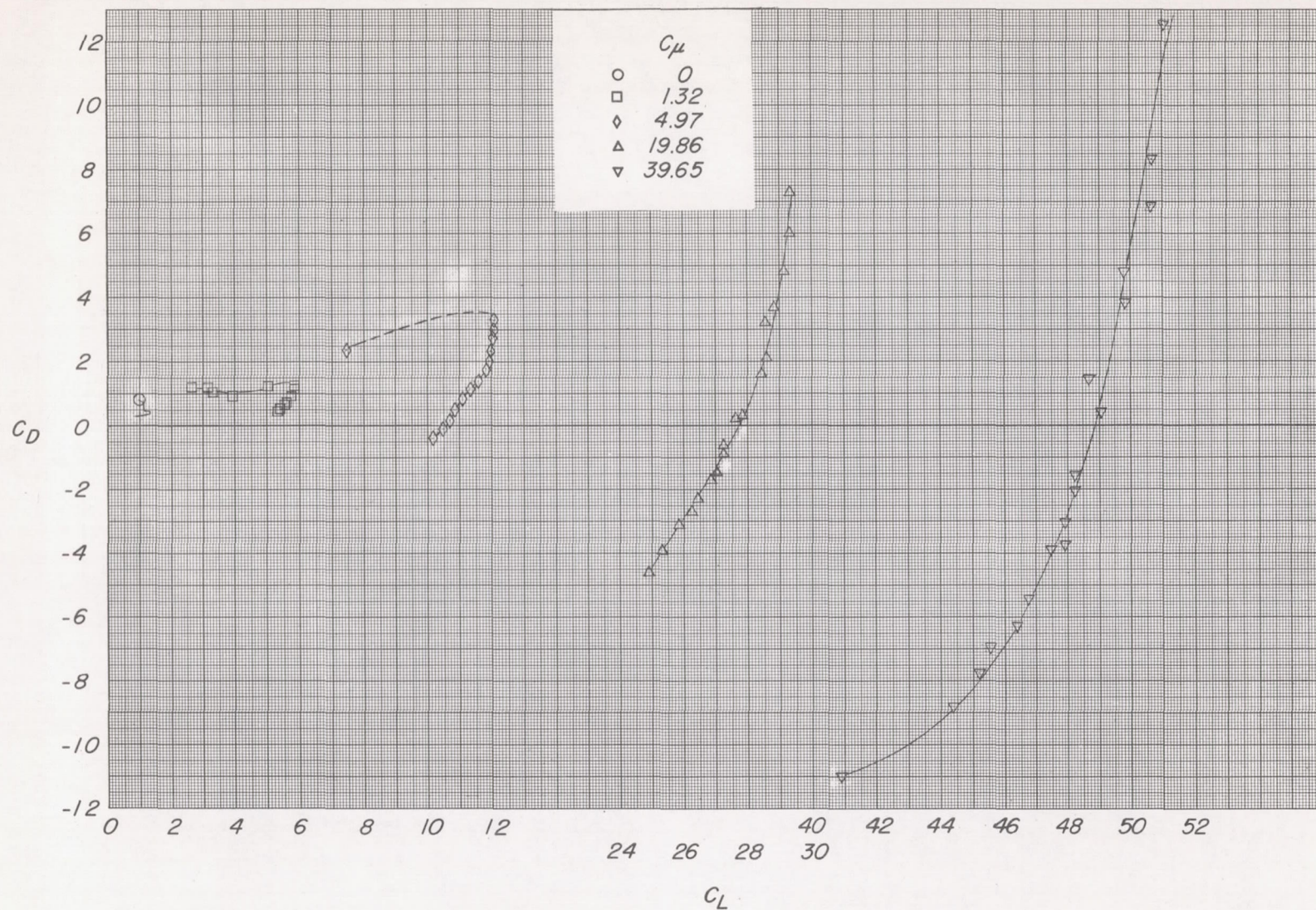
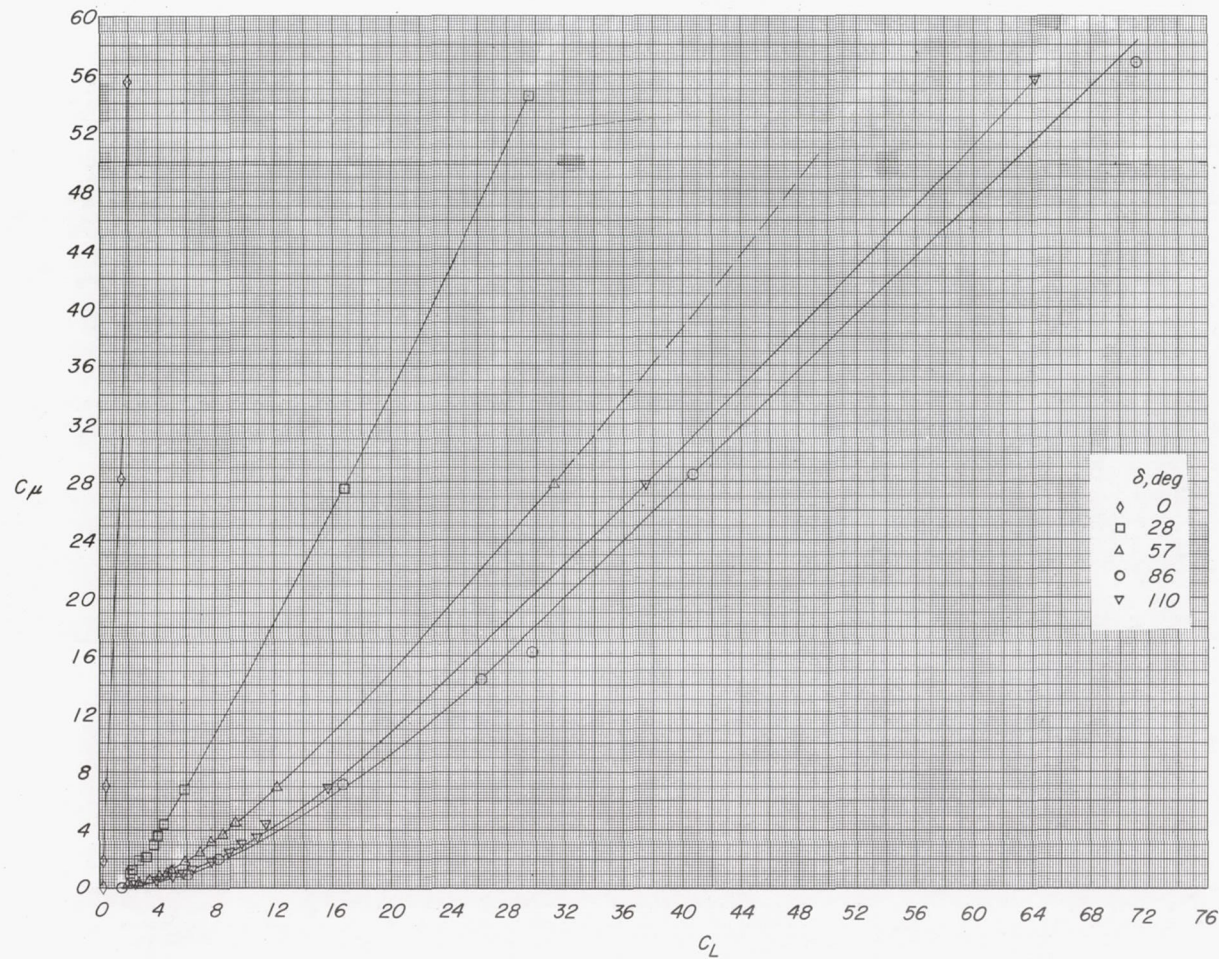
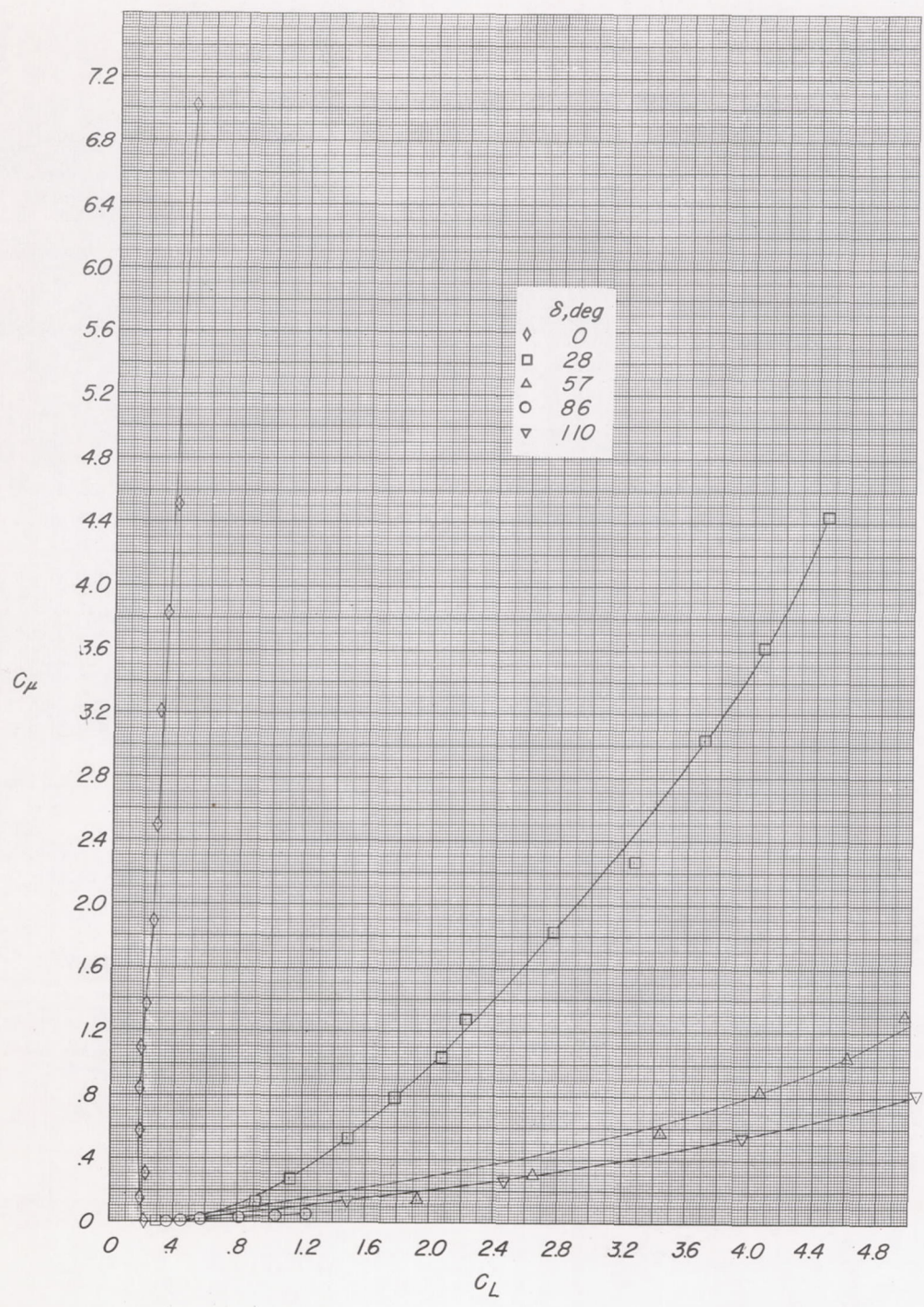


Figure 11.- Concluded.



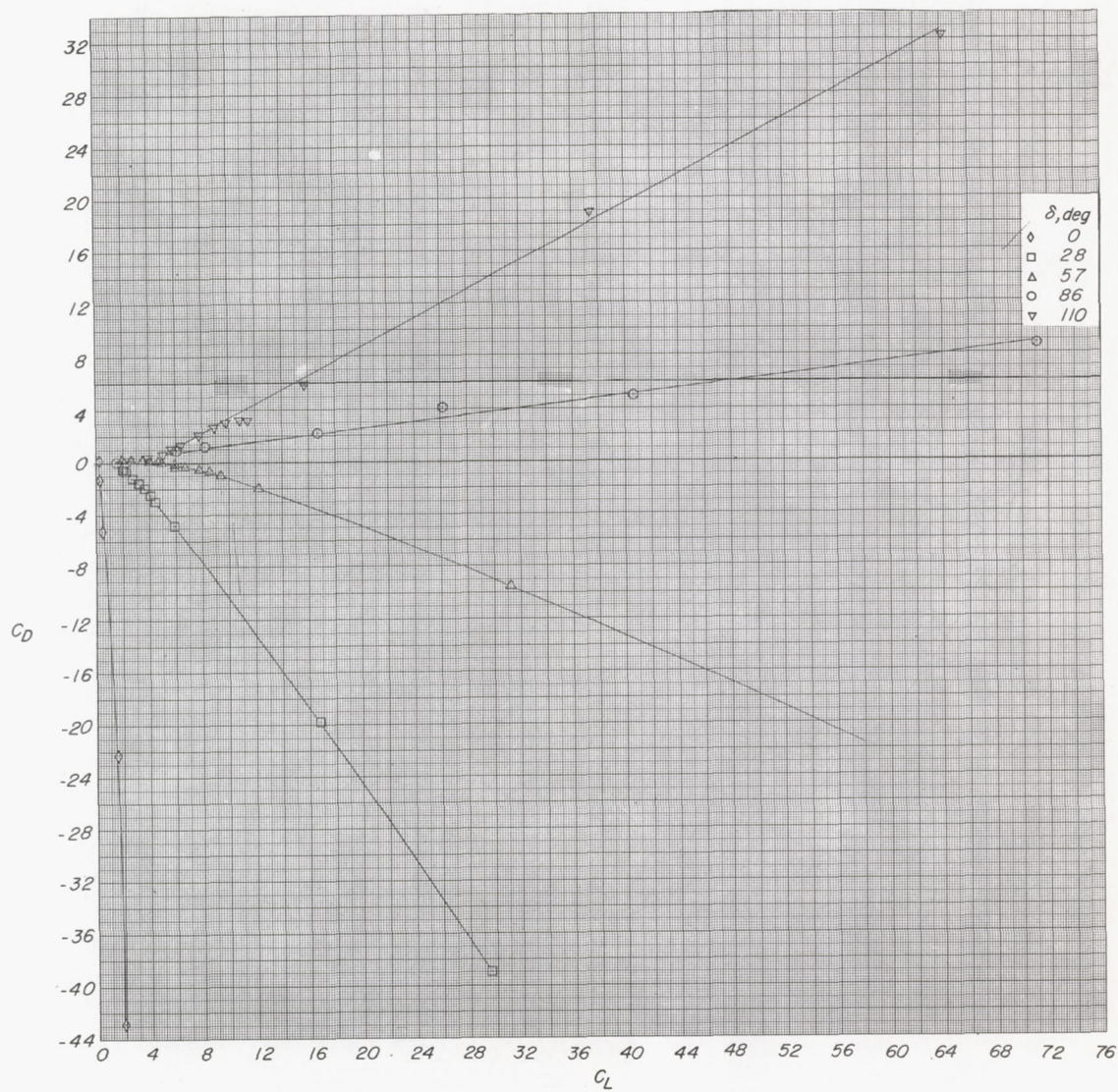
(a) C_μ against C_L.

Figure 12.- Variation of the aerodynamic characteristics with momentum coefficient for the jet flap at α = 0°.



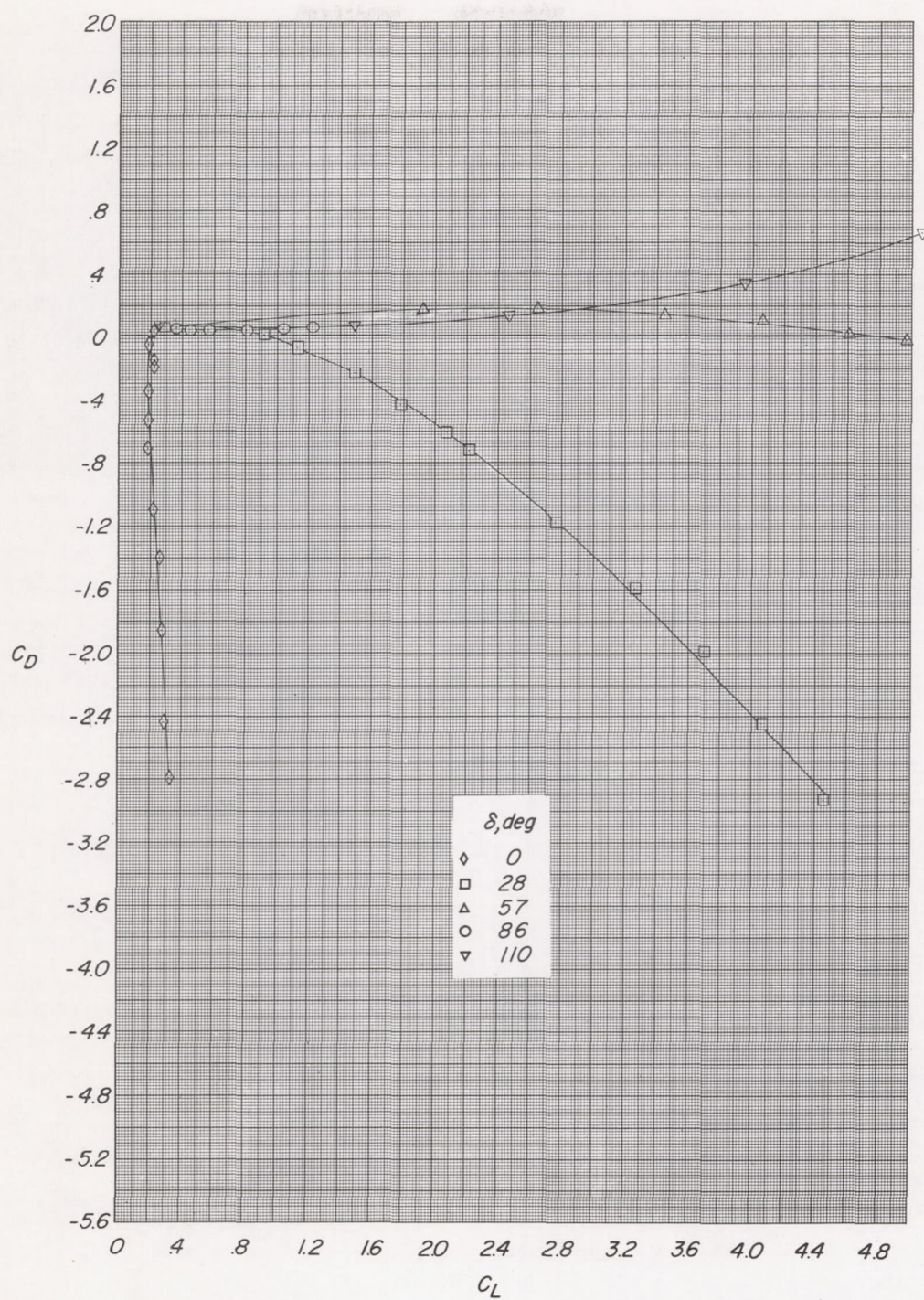
(a) Concluded.

Figure 12.- Continued.



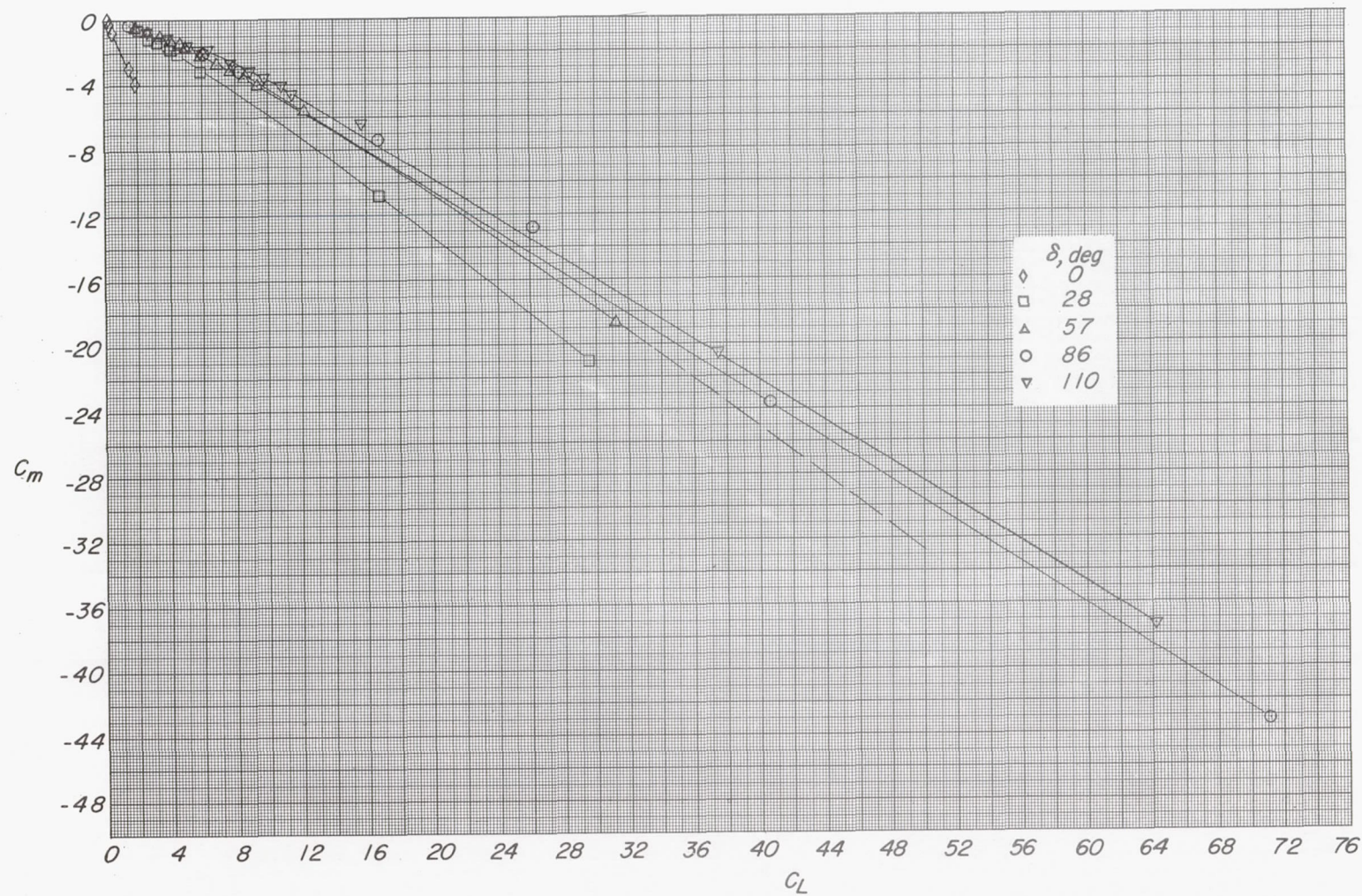
(b) C_D against C_L .

Figure 12.- Continued.



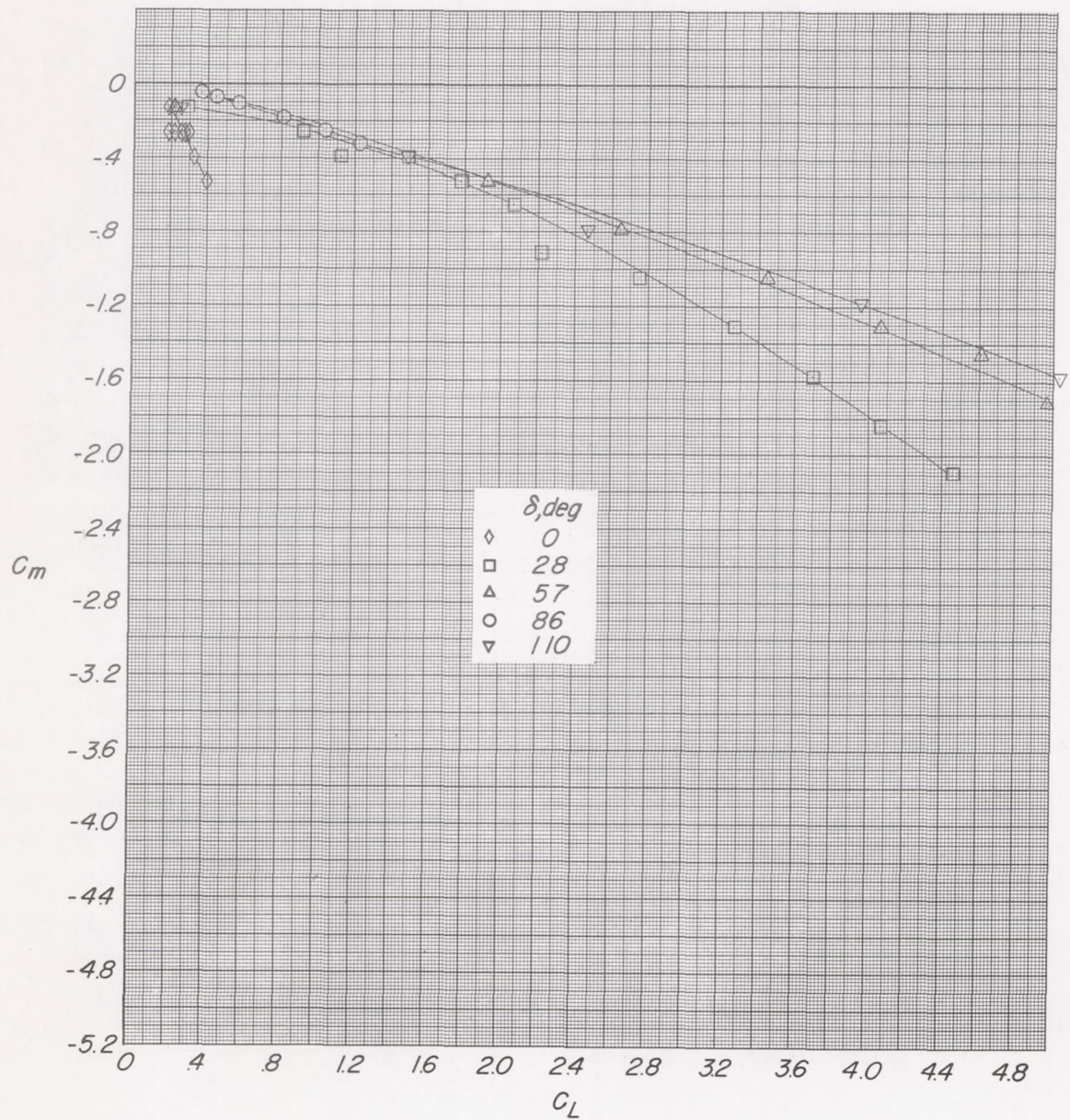
(b) Concluded.

Figure 12.- Continued.



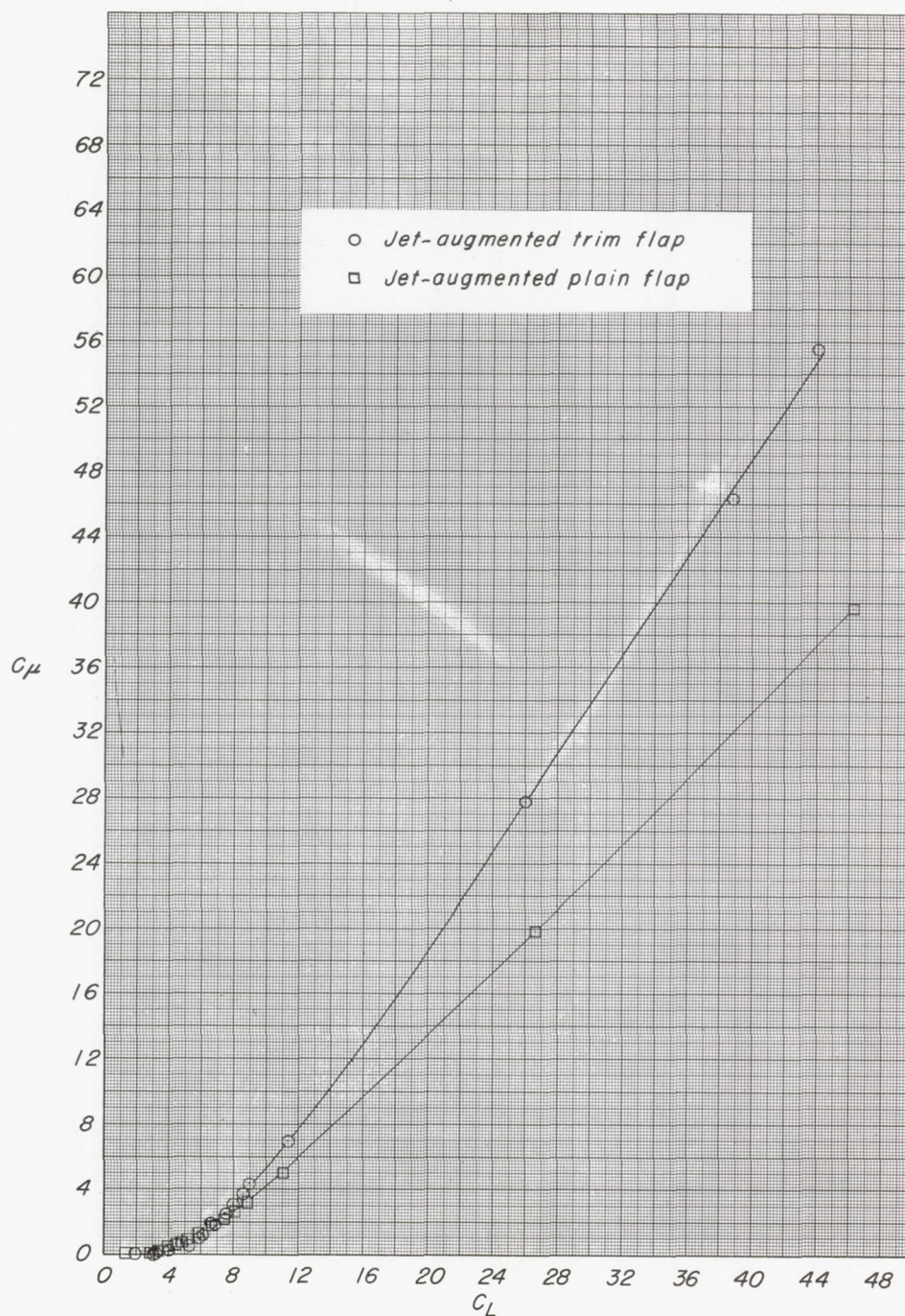
(c) C_m against C_L .

Figure 12.- Continued.



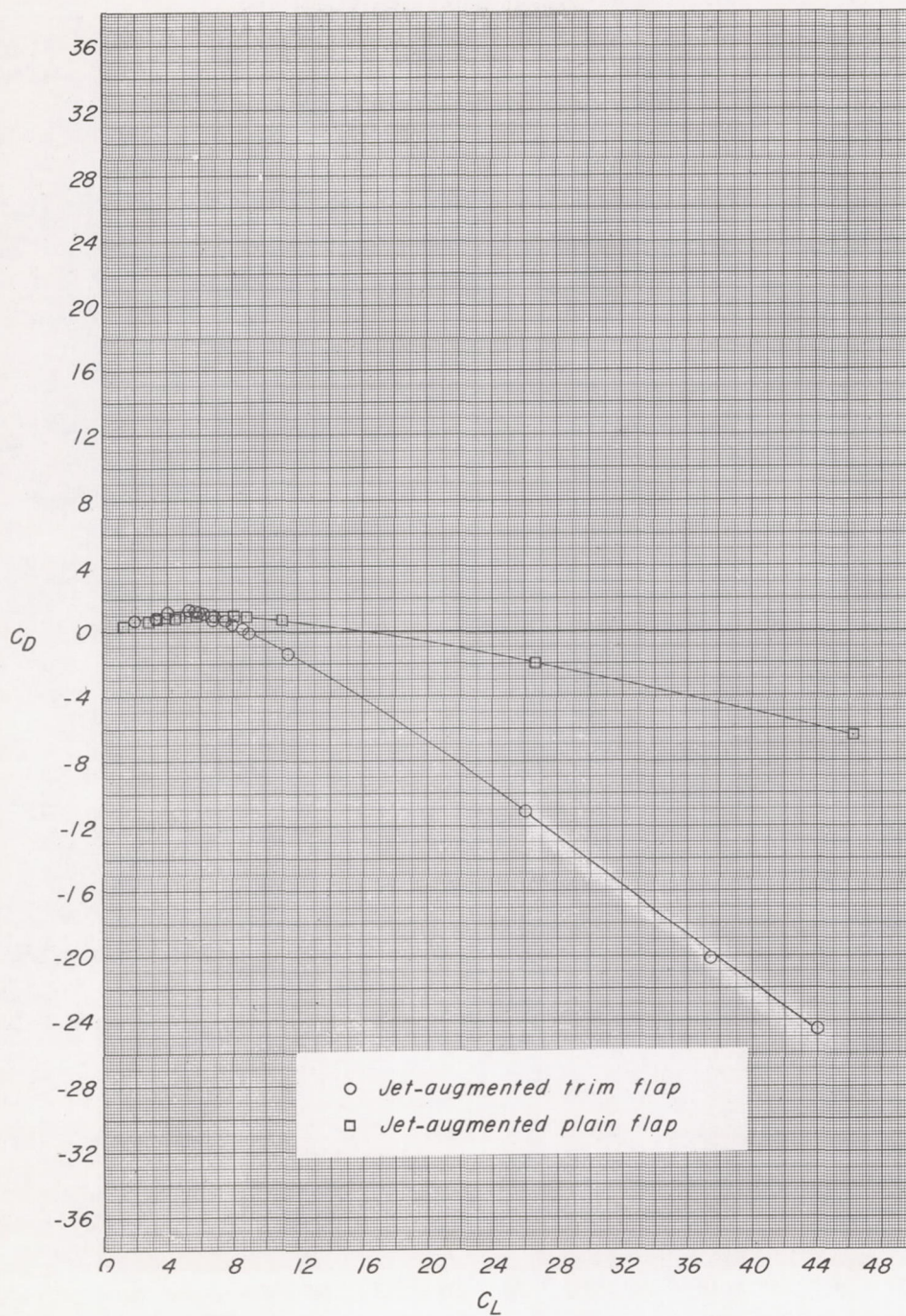
(c) Concluded.

Figure 12.- Concluded.



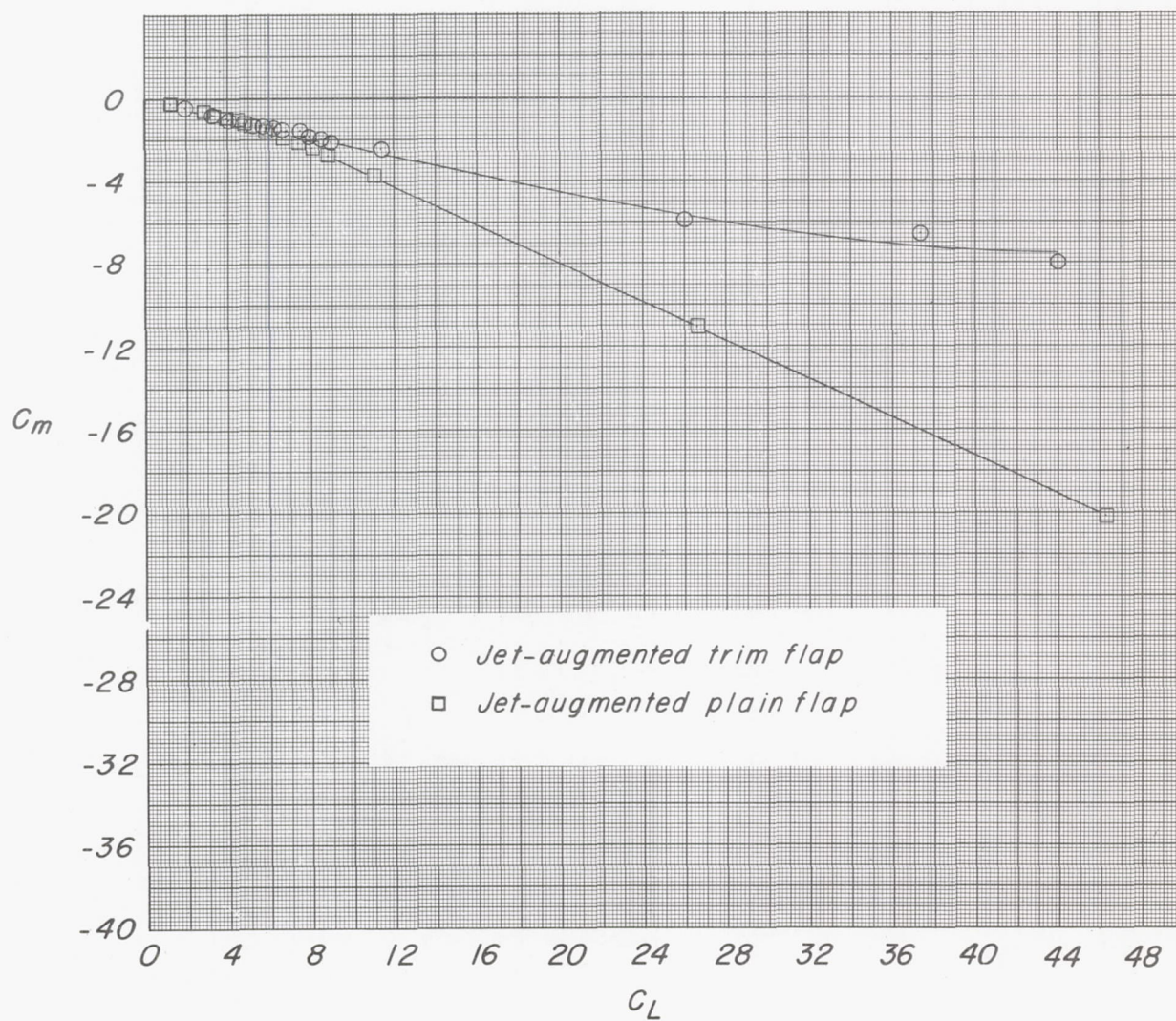
(a) C_μ against C_L .

Figure 13.- Variation of the aerodynamic characteristics with momentum coefficient for the jet-augmented plain flap ($\delta = 67^\circ$) and jet-augmented trim flap ($\delta = 40^\circ$) at $\alpha = 0^\circ$.



(b) C_D against C_L .

Figure 13.- Continued.



(c) C_m against C_L .

Figure 13.- Concluded.

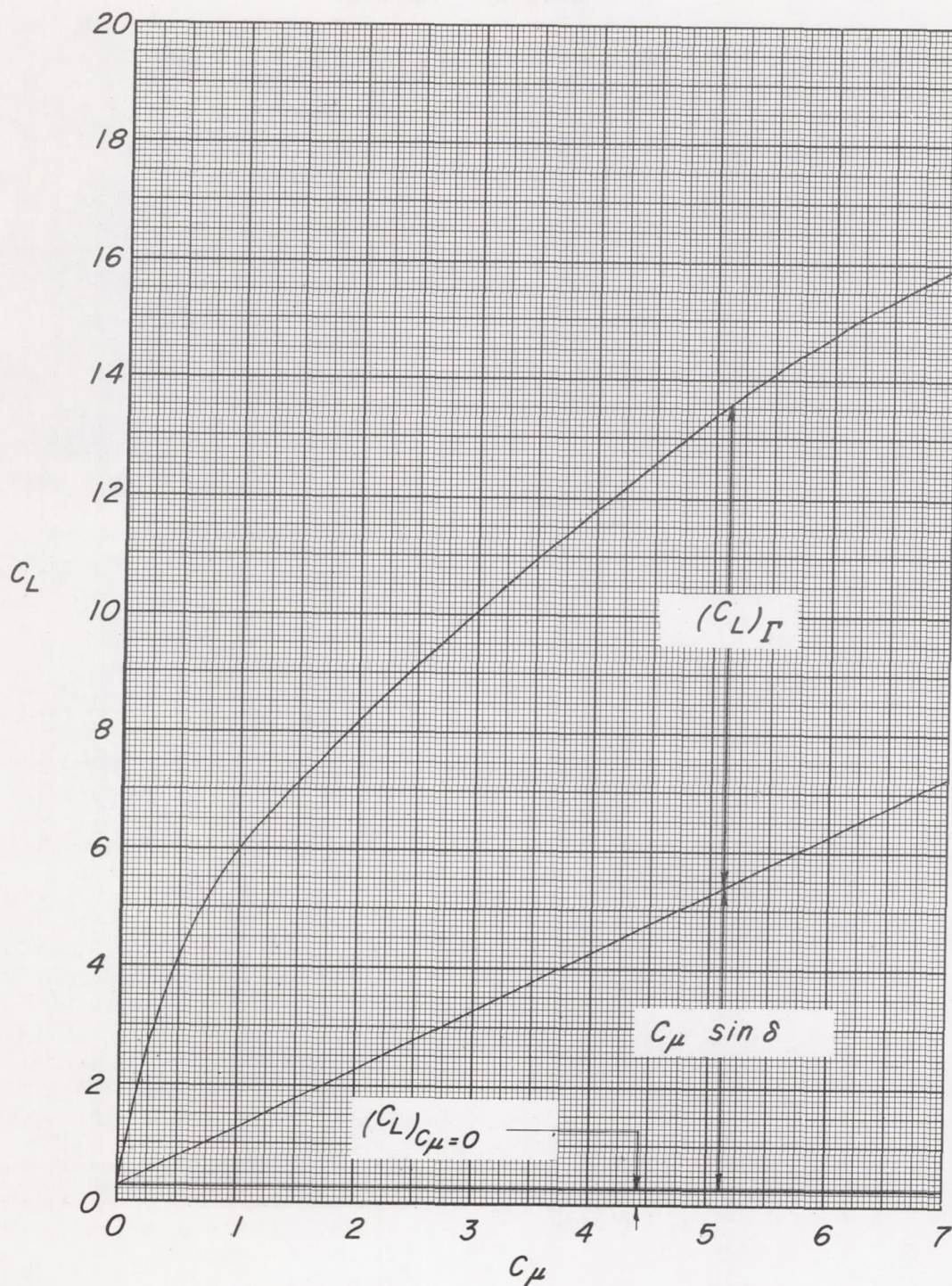


Figure 14.- Factors making up the lift coefficient of the jet flap.
 $\alpha = 0^\circ$; $\delta = 86^\circ$.

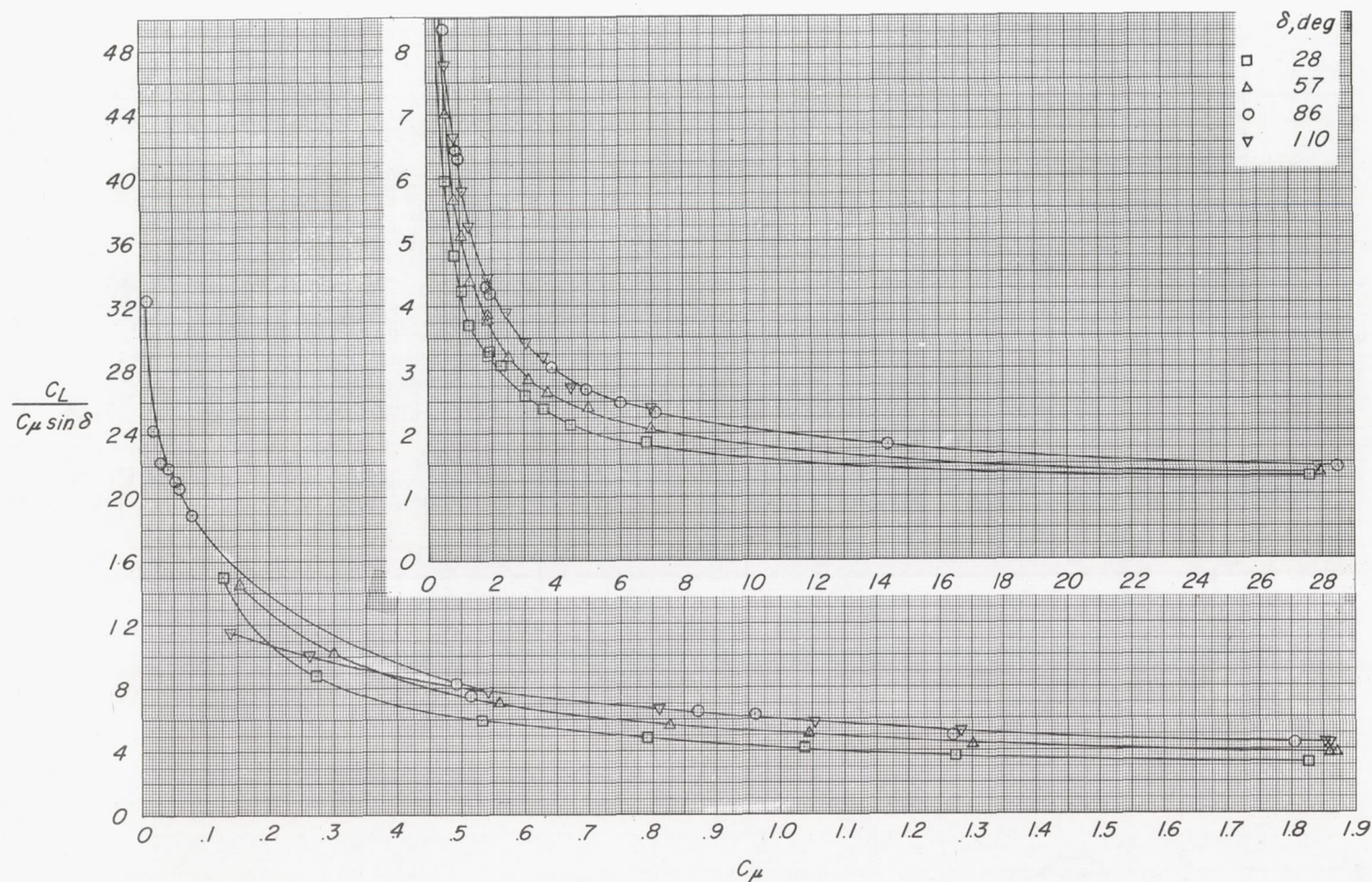


Figure 15.- Variation of the magnification factor $\frac{C_L}{C_\mu \sin \delta}$ with momentum coefficient for the jet flaps at $\alpha = 0^\circ$.

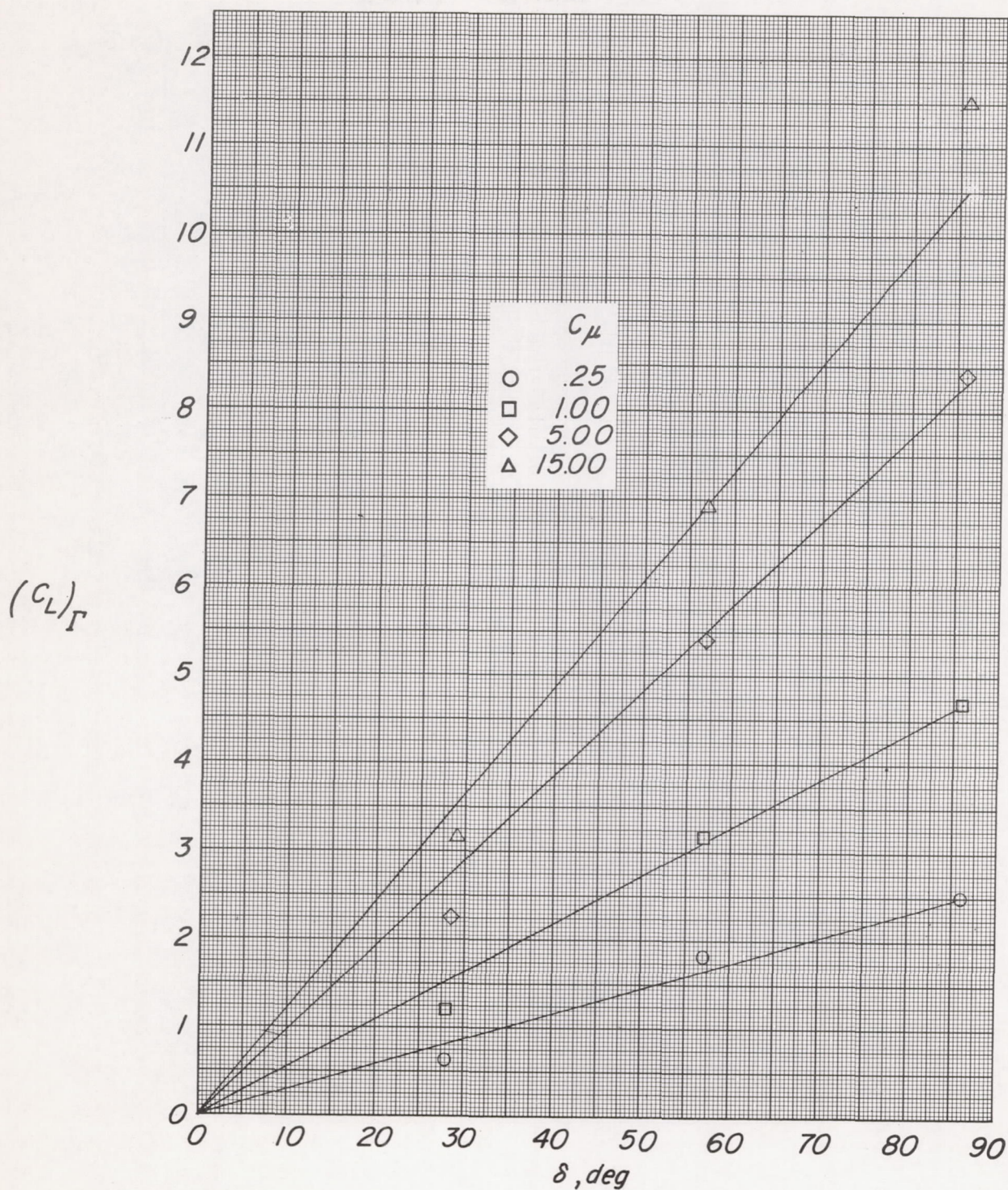


Figure 16.- Variation of jet-circulation lift coefficient with jet-deflection angle. $\alpha = 0^\circ$.

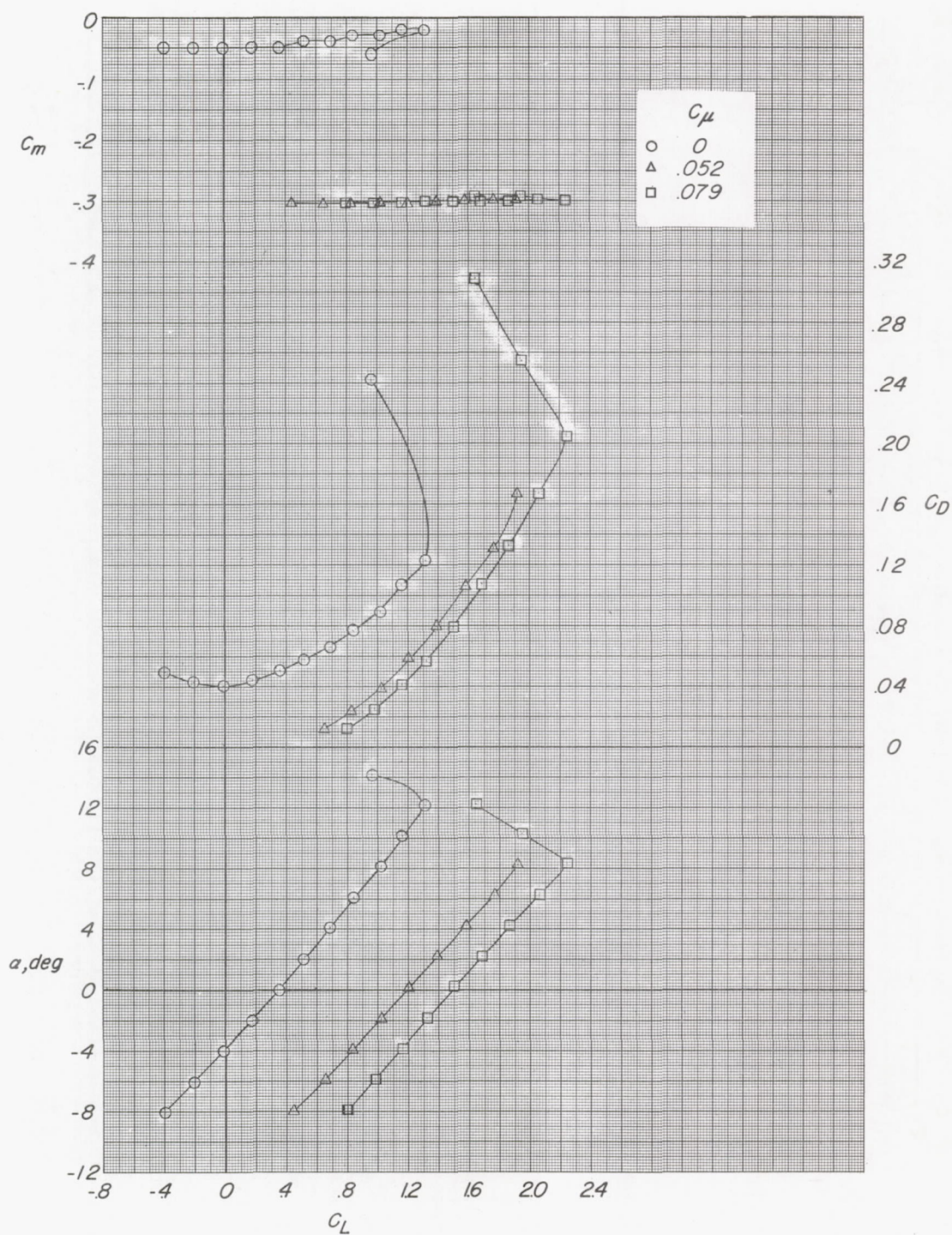


Figure 17.- Aerodynamic characteristics in pitch of the jet flap at high dynamic pressures. $\delta = 86^\circ$.

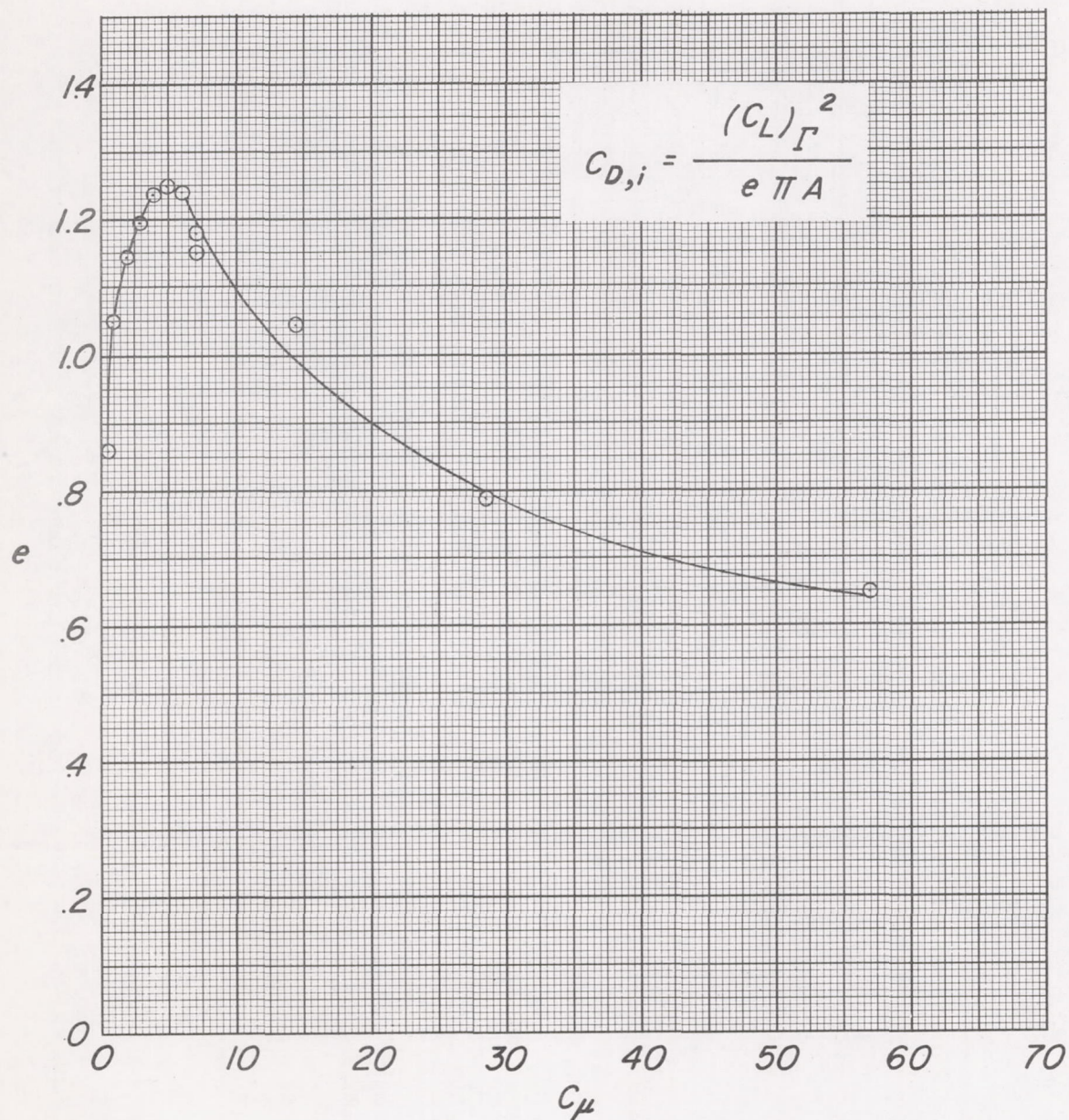


Figure 18.- Variation of induced-drag efficiency factor e with momentum coefficient. $\alpha = 0^\circ$; $\delta = 86^\circ$.

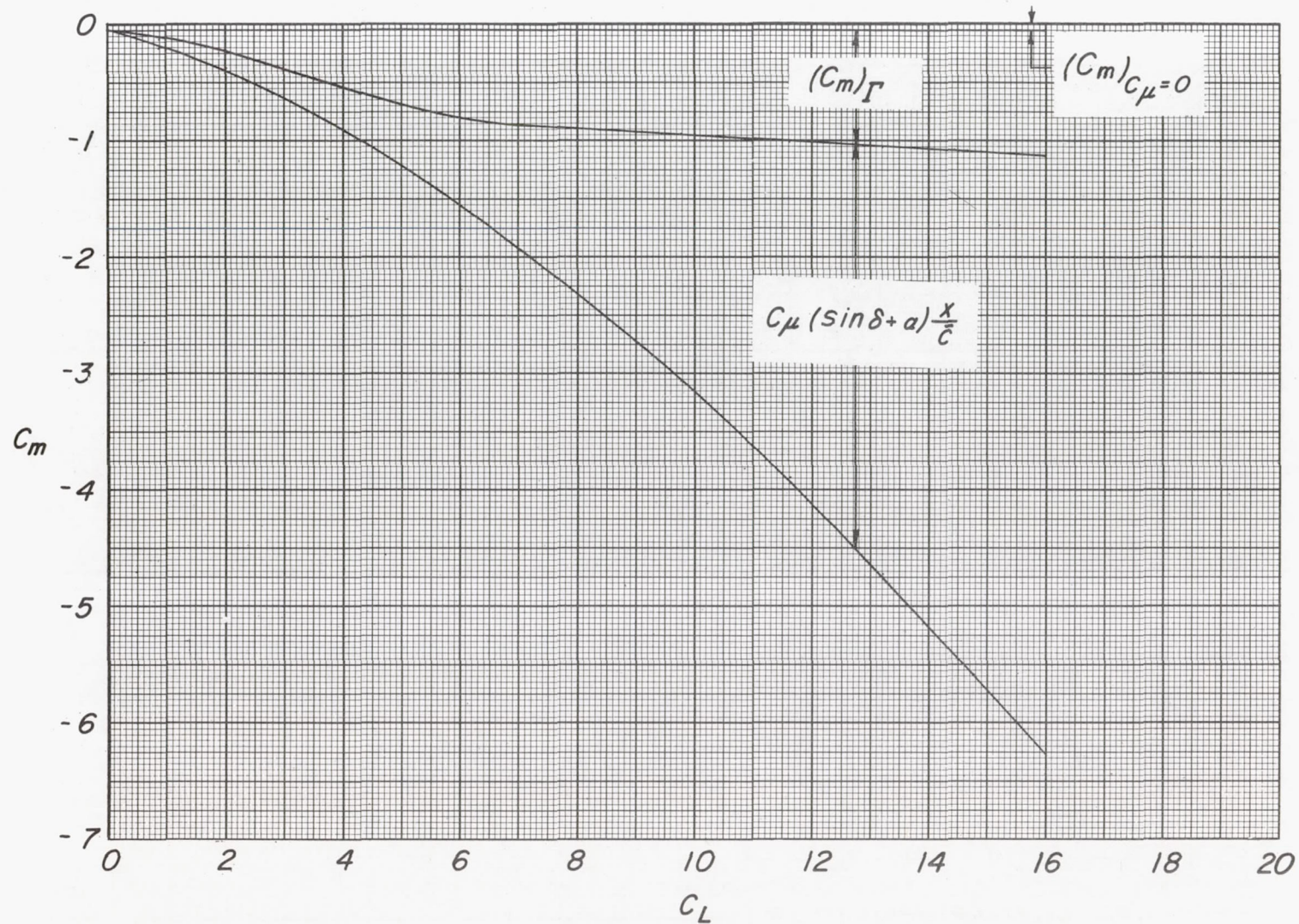


Figure 19.- Factors making up the pitching-moment coefficient of the jet flap. $\alpha = 0^\circ$; $\delta = 86^\circ$.

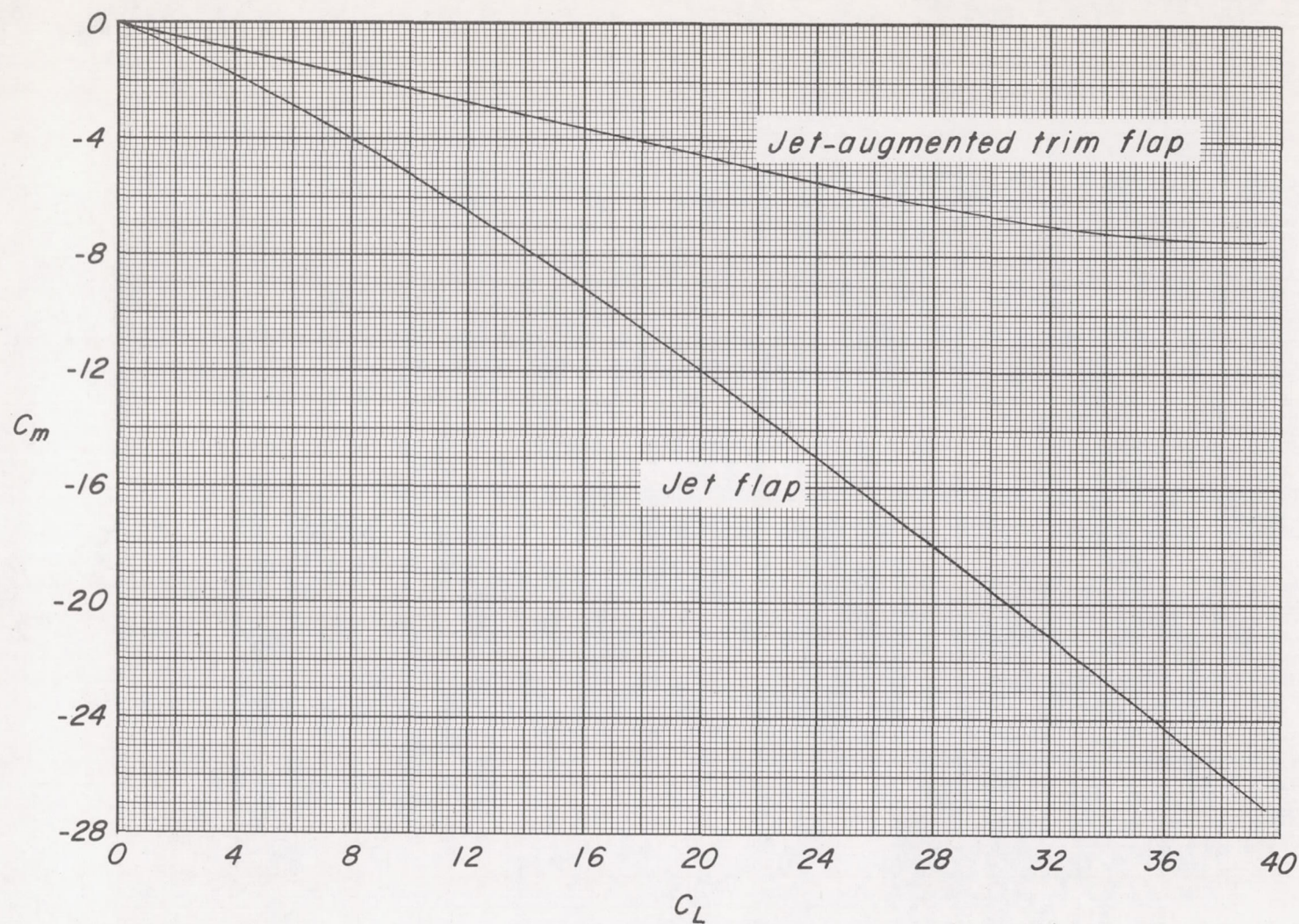


Figure 20.- Comparison of the pitching-moment coefficients of the jet flap and the jet-augmented trim flap. $\alpha = 0^\circ$; $\delta = 40^\circ$.

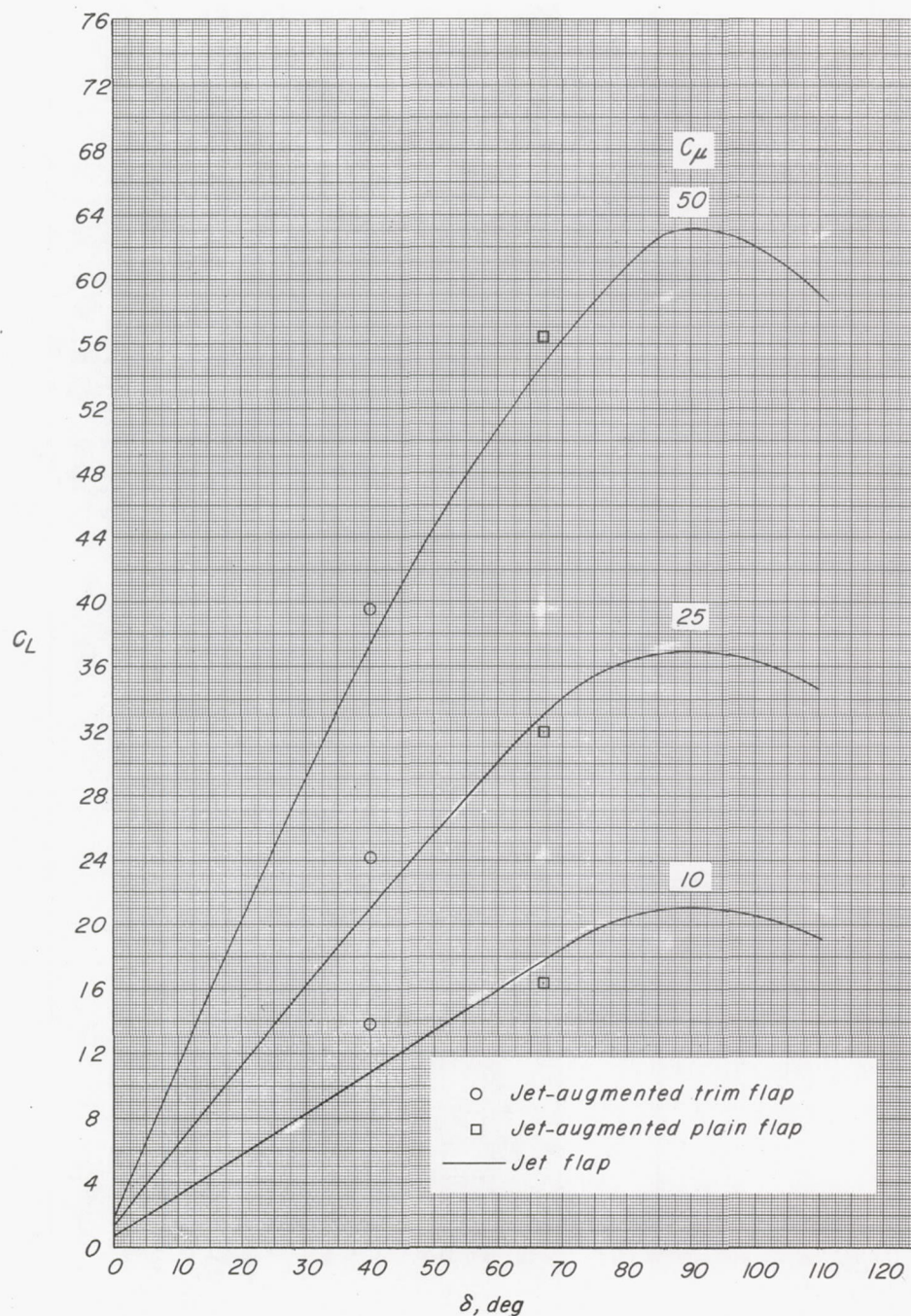
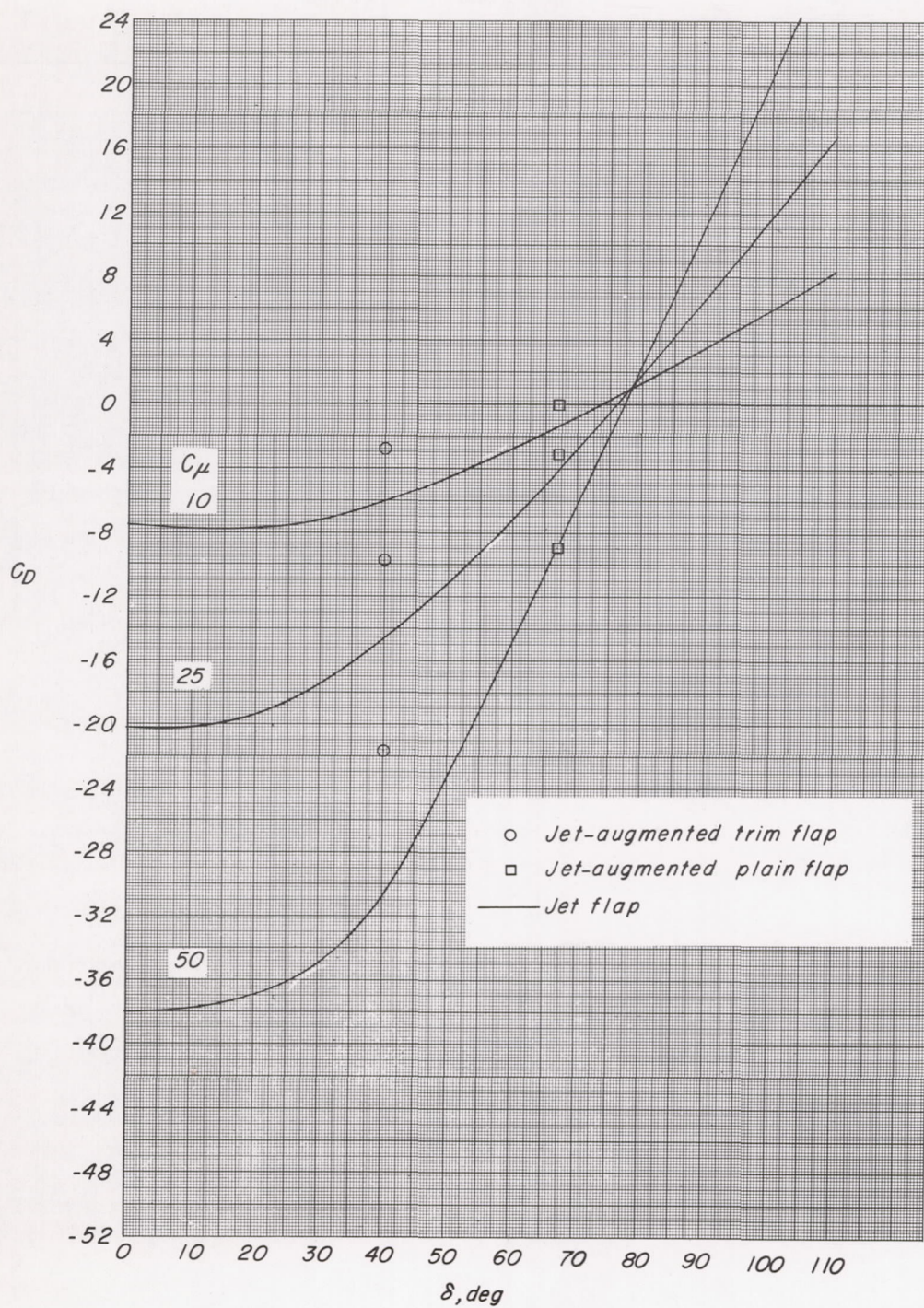
(a) C_L against δ .

Figure 21.- Variation of aerodynamic characteristics with jet-deflection angle for three values of momentum coefficient at $\alpha = 0^\circ$.



(b) C_D against δ .

Figure 21.- Continued.

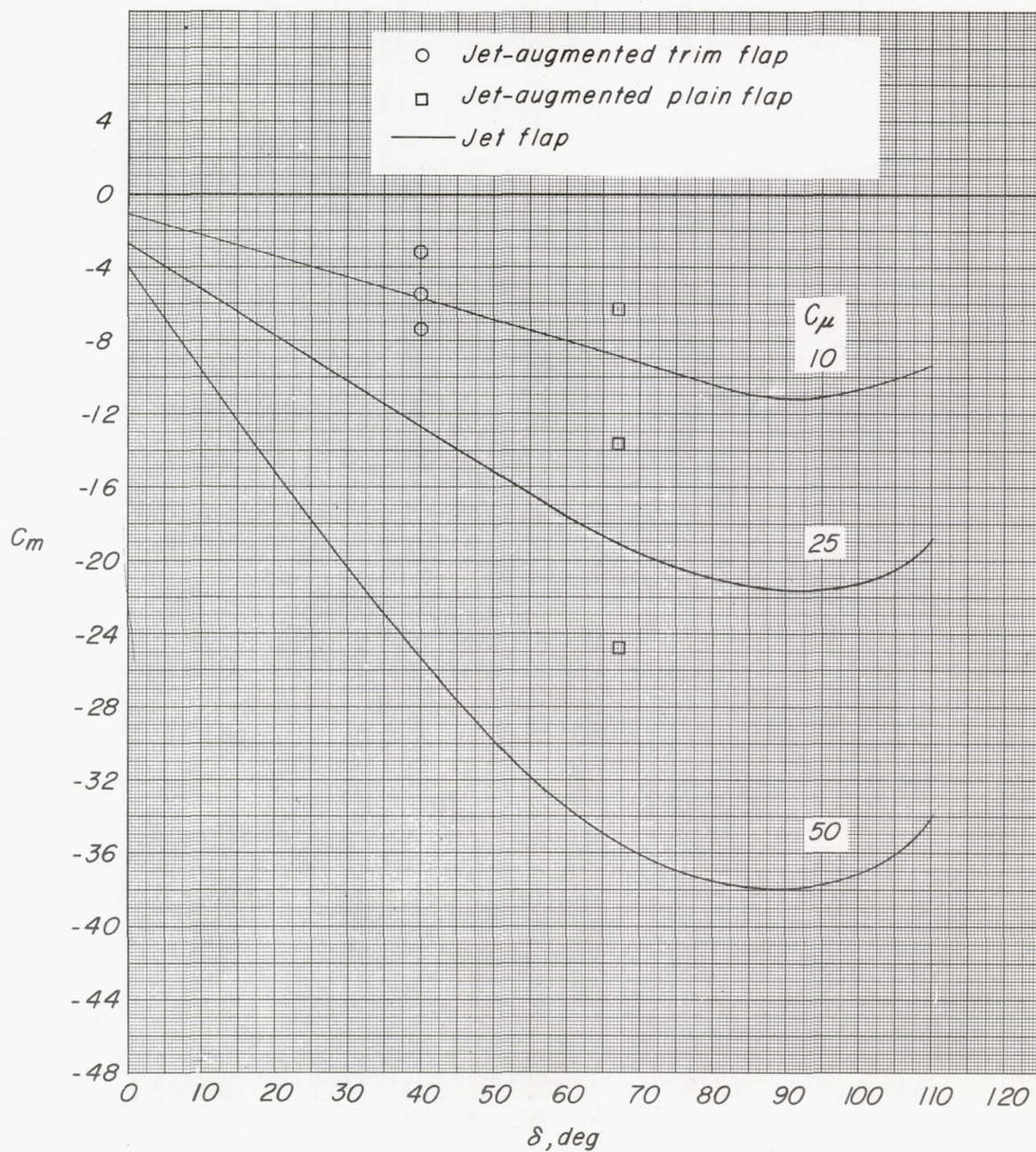
(c) C_m against δ .

Figure 21.- Concluded.

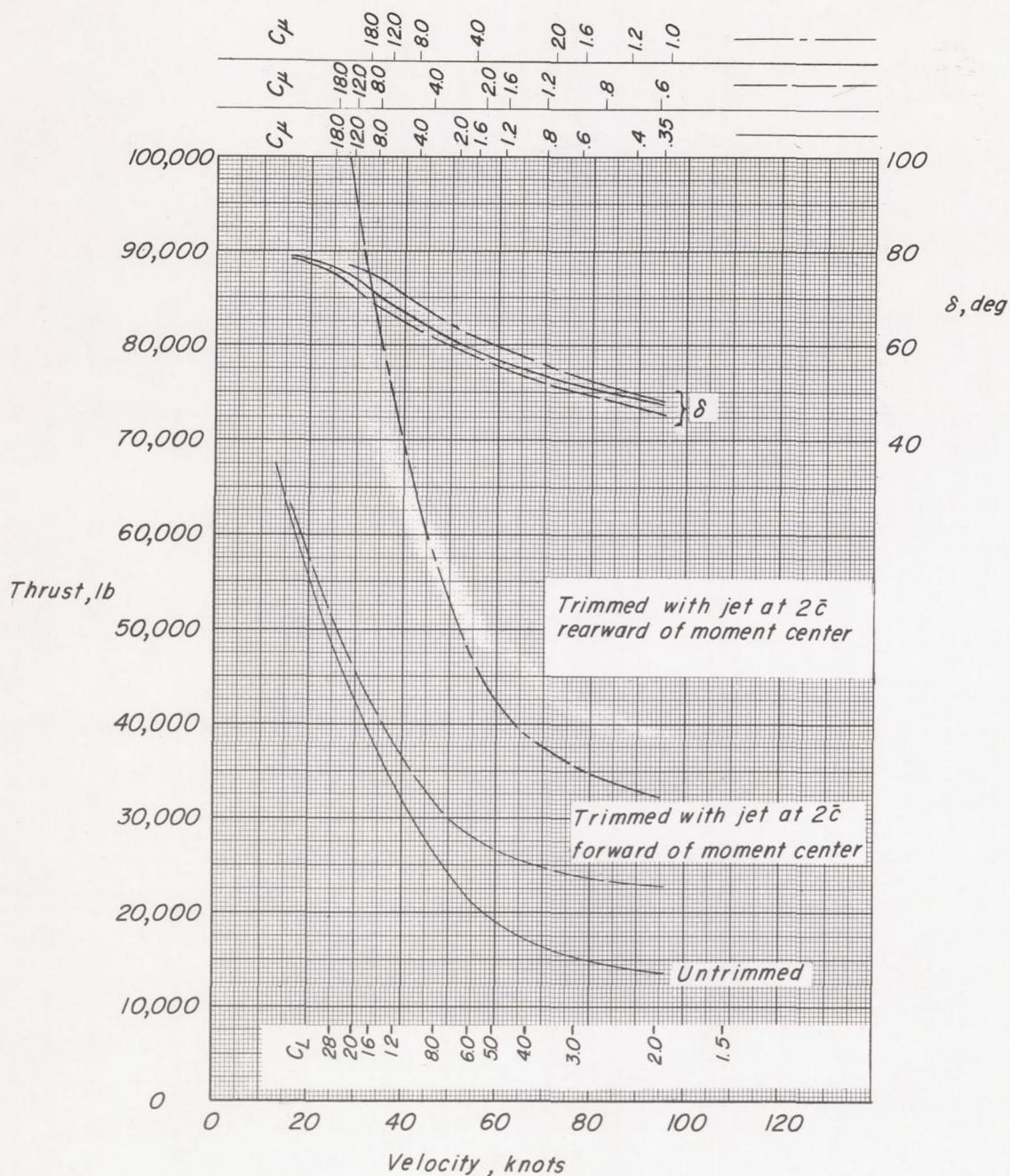


Figure 22.- Estimation of thrust and jet-deflection angles required for a hypothetical airplane using the jet-flap system with a wing loading of 60 pounds per square foot, a weight of 75,000 pounds, and $\alpha = 0^\circ$.